Multi-objective process optimisation of beer fermentation via dynamic simulation

Multi-objective process optimisation of beer fermentation via dynamic simulation

Alistair D. Rodman, Dimitrios I. Gerogiorgis*

School of Engineering, University of Edinburgh, The King's Buildings, Edinburgh, EH9 3JL, UK

*****Corresponding author: D.Gerogiorgis@ed.ac.uk (+44 131 651 7072)

ABSTRACT

Fermentation is an essential step in beer brewing: when yeast is added to hopped wort, sugars released from the grain during germination are fermented into ethanol and higher alcohols. To study, simulate and optimise the beer fermentation process, accurate models of the chemical system are required for dynamic simulation of key component concentrations. Since the entire beer production process is a highly complex series of chemical reactions with the presence of over 600 species, many of the specific interactions are not quantitatively understood, a comprehensive dynamic model is impractical.

This paper presents a computational implementation of a detailed model describing an industrial beer fermentation process, which is used to simulate published temperature manipulations and compare results with those obtained following the protocol currently in place at WEST Beer brewery (Glasgow, Scotland, UK). A trade-off between design objectives has been identified, making determination of a single optimal scenario challenging. A Simulated Annealing (SA) algorithm has been developed in order to pursue stochastic optimisation of the fermentor temperature manipulation profile, on the basis of generating an enormous set of plausible manipulations which adhere to suitable operability constraints at an appropriate level of temporal domain discretisation. The objective function considers ethanol maximisation as well as batch time minimisation (with variable weight allocation), and explicit constraints on diacetyl and ethyl acetate concentrations. Promising temperature manipulations have been determined, allowing for batch time reductions of as high as 15 hours: this represents a substantial decrease in production cycle time, and is thus expected to improve annual plant throughput and profitability, without any discernible effect on flavour.

1. INTRODUCTION

1.1 FERMENTATION

The production of beer is well documented, with suggestions that it is one of the world's oldest prepared beverages, dating as early as the early Neolithic period (Arnold, 1911). Today beer is the most widely consumed alcoholic beverage in the world (Rehm et al., 2003) with the global beer market estimated to be over 500 billion USD in 2015 (Markets, 2013). The continual growth of the alcohol industry as a whole has resulted in an ever-increasing demand for beer products, with a rapid increase in the demand for super premium and craft beer products observed in the last 5 years. Market competitiveness makes it imperative that brewers operate their production processes effectively: the ability to improve any stage of production will have a significant effect on profitability and the ultimate success or failure of a brewery.

While many variations of the beer manufacturing process exist, industrial production almost invariably follows the scheme outlined in Fig. 1. Beer production is a complex chemical process: nevertheless, its only prerequisite is the use of the same four essential ingredients: a starch source, yeast, hops and water (Southby, 1885).

Beer production requires few raw materials and many rudimentary processing techniques, however what is produced is a highly complex mixture of chemical species which govern product quality and flavour. It is the varying combinations of these compounds which are responsible for the unique taste of each beer brand, however many are unpleasant at certain concentrations. Diacetyl (2,3-butanedione) has a pungent butter-like aroma (Izquierdo-Ferrero et al., 1997), similar to banana flavouring agents (Hanke et al., 2010), and is often produced well above the flavour threshold in brewing. Due to their volatility, esters also contribute significantly to beer aroma; ethyl acetate is often used as an indicator of all esters present, and is described as having the odour of nail varnish remover. It is essential that efforts to improve fermentation efficacy are mindful of the degrading effect which these compounds have on product quality, if present in substantial quantity.

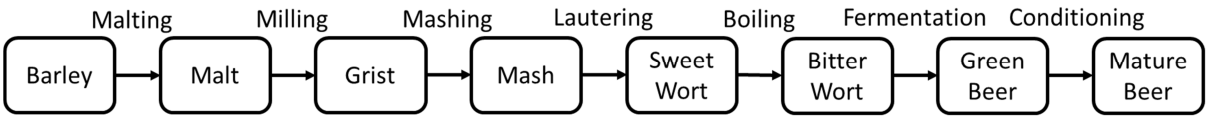

Figure 1. Block flow diagram of the beer production process.

1.2 FERMENTATION

Fermentation is an essential brewing process unit operation, and the focus of this study. Yeast is introduced once the cooled wort (a sugar rich brewing intermediate, Hough et al., 1982) from the boiling process (Hudson and Birtwistle, 1966) enters fermentation vessels (*pitching*). The primary chemical reaction pathway is the conversion of two sugar molecules into one ethanol and one carbon dioxide molecule, which is coupled with biomass growth and exothermic reaction heat generation. Concurrently, a wide range of species are formed at low concentrations by a multitude of side reactions, many of which contribute to beer flavour.

Fermentation progression is sensitive to yeast pitching rate (Guido et al., 2004), dissolved oxygen content, batch pressure and system temperature, which strongly affects yeast growth and metabolic rate: as long as yeast cells are not damaged and are kept below 30 ºC, high temperature accelerates fermentation. Nevertheless, ethanol and volatile flavour component loss rates are too severe at higher temperatures, coupled with increased production of undesirable aromatic compounds and bacterial growth promotion. Therefore, brewers control temperature inside the fermenter as the batch progresses, to accelerate fermentation while ensuring that yeast is not denatured and that no undesired by-product species are produced.

Online measurements can be cumbersome: each beer brand or line may have a proprietary temperature manipulation profile used for every batch, to ensure product consistency (Trelea et al., 2001). Offline measurements to assess fermentation progression are often limited to wort density or specific gravity. The Plato (specific gravity) scale represents equivalent sucrose concentration: sugar depletion is a useful indicator of the extent of fermentation. A primary concern of the brewing industry is the selection and implementation of an appropriate dynamic temperate profile throughout the fermentation process, to ensure high product quality, eliminate batch variations and ensure brand consistency and customer satisfaction.

Fermentation duration varies by product sought. Lagers are fermented at temperatures around 10 ºC, requiring a fermentation time of about a week. Ales are fermented at higher temperatures (22 ºC) and thus require 3-4 days (Boulton and Quain, 2008). Given the diversity of brewing operations around the world, many vessel types are used for fermentation. Typically, fermentation tanks are cylindro-conical stainless steel vessels. This shape promotes the circulation of CO_2 bubbles to agitate and mix the contents (which are not agitated or circulated by any mechanical means), helping to maintain a uniform vessel

temperature. Moreover, it facilitates recovery of settled yeast from the cone, for lager-producing bottom yeasts. Conversely, ale-producing top yeasts settle at the free surface of the vessel and can be skimmed off. Fermentation tanks typically feature a cooling jacket, used to control the wort temperature in order to follow the brewer's desired profile. Larger tanks may include separate cooling mechanisms on the conical and cylindrical portions, allowing control of the internal circulation pattern (Boulton & Quain, 2008).

1.3 SUMMARY & OBJECTIVES

Fermentation is an essential part of beer production; the process is time-consuming and energy-intensive, so the effort to shorten its duration and cost implies enormous potential savings. The chemical system is highly complex, and all concurrent chemical reactions during fermentation have an extremely significant effect on the resulting product flavour. Therefore, efforts to improve process efficiency must explicitly consider the effect of any process modification on the product quality. While beer brewing is an established industry, the system complexity induces a lack of understanding of much of the chemical phenomena taking place, making it extremely challenging to explicitly predict the effect of process alterations on the required processing time and product composition.

The present study is aimed at beer fermentation modelling toward recommending process operation improvements for an industrial partner, WEST Beer (Glasgow, UK). Published kinetic models have been reviewed and a detailed dynamic model has been used to simulate the WEST fermentation process, enabling comparison of dynamic model predictions and current industrial operating practice: improved operating procedures have been systematically determined toward reducing beer fermentation time while maintaining high product quality.

2. REVIEW OF PUBLISHED MODELS AND OPTIMISATION

Computational prediction and performance assessment of a biochemical process toward process optimisation requires a mathematical model representing species consumption and production. Given the complexity of the fermentation process, and the numerous (over 600) species present (Vanderhaegen et al., 2006), many chemical interactions are not quantitatively understood and the construction of a comprehensive dynamic process model is thus infeasible. Reduced-order dynamic fermentation models considering only the key chemical reaction pathways, using parameters computed from experimental campaign data.

The extreme industrial importance of dynamic modelling for high-fidelity simulation and optimisation of fermentation processes is not confined to brewing only. Achieving high efficiency is vital in producing a wide array of therapeutic molecules (especially antibiotics), so process intensification is of enormous interest, particularly in the context of continuous pharmaceutical manufacturing (Gerogiorgis and Barton, 2009; Schaber et al., 2011; Jolliffe and Gerogiorgis, 2015a, 2015b).

2.1 BATCH FERMENTATION KINETIC MODELS

The earliest kinetic model of beer fermentation has been published by Engasser et al. (1981), based on fundamental biochemical pathways and the manner in which the evolution of alcohol and sugars depends on total biomass (yeast) concentration. Gee and Ramirez (1988) adapted this work to include temperature effects on rate expressions. The model considers 3 ordinary differential equations (ODEs) predicting consumption of glucose, maltose and maltotriose (assumed to be the limiting nutrients) via Monod kinetics.

Gee and Ramirez (1994) also published a subsequent paper to extend the model and consider further compounds, while also incorporating a simple feedback inhibition mechanism on cell growth rate. The model considers a total of twelve species affecting product flavour, in addition to the five described in the original growth model (Gee and Ramirez, 1988), however new parameters are only stated for isothermal conditions.

De Andrés-Toro et al. (1998) proposed an alternative kinetic model for beer production under industrial operating conditions. Unlike the model of Gee and Ramirez which is based on sugar uptake rate, this later model relies on predicting yeast evolution in order to subsequently compute chemical species growth. Five responses are considered; ethanol, sugar, biomass and two flavour-contributing compounds (diacetyl and ethyl acetate). Here, the single sugar compound represents the sum of all sugars present in the wort. The suspended biomass within this model is distinguished into three distinct types; active, latent and dead cells. Latent (lag) cells cannot promote fermentation: over time, they are transformed into active cells, responsible for consumption of fermentable sugars. Active cells duplicate and grow over time, but a portion of them will die, settle and no longer contribute to fermentation.

The fermentation process is distinguished into two observable phases; in the first (lag phase), the majority of biomass introduced comprises of latent yeast cells, so minimal fermentation takes place as latent cells undergo activation. Once approximately half of the

suspended cells are activated, the second (fermentation phase) begins: therein, active cell concentration is sufficient to induce the enzymatic effect, converting the sugar substrate to ethanol product. An overview of the biomass scheme is given in Fig. 2a. Evolution of each cell type is predicted by the respective ODE, where growth rates are Arrhenius temperature functions of the corresponding species maximum growth rate. This allows the total suspended cell (lag, active and dead) population growth to be defined as the rate of active cell growth minus the rate of dead cells settling. Sugar consumption is related to active biomass concentration with its own growth rate: ethanol production is predicted similarly, but with an inhibition factor used to account for its decreasing production rate with time. Ethyl acetate production is related to sugar consumption with a stoichiometric factor as in the Gee and Ramirez model (1994), which however includes explicit temperature dependence. Diacetyl growth modelling is more elaborate: the respective ODE includes two terms, one accounting for its production early in the fermentation process and another representing its consumption toward partial conversion to 2,3-butanediol during fermentation progression.

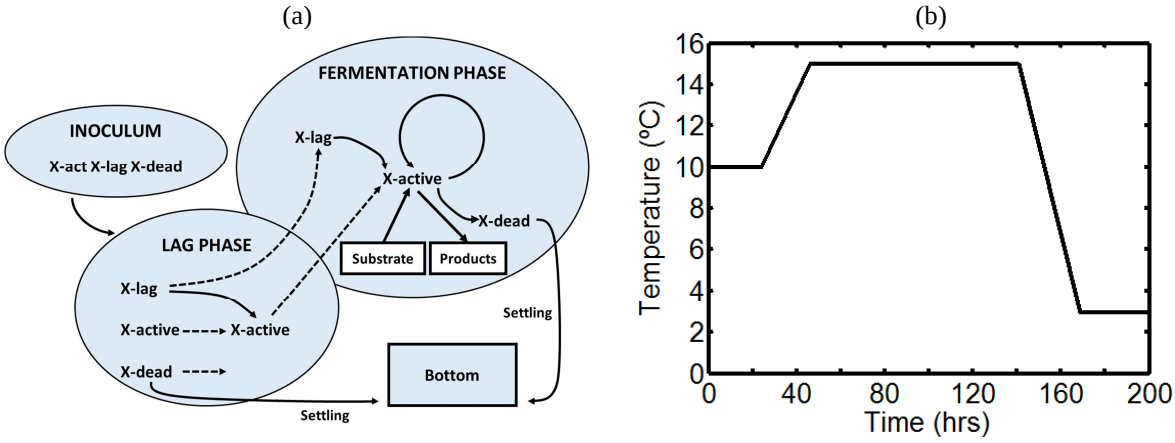

Figure 2. (a) Process scheme considered in the kinetic model. (b) Generic industrial temperature profile.

The seven ODEs of the model depend on 10 parameters which vary with temperature and have been modelled using Arrhenius relationships and parameter values estimated from experimental data. Isothermal fermentations have been carried out in a lab-scale 3 L vessel at 5 different temperatures in order to obtain online measurements of species concentrations. Following model parameter estimation, the authors performed a non-isothermal fermentation in a pilot plant-scale 100 L tank using a generic industrial temperature profile (Fig. 2b). Published profile predictions are in good agreement with the pilot-plant experimental data;

the validated model has been successful in predicting process behaviour in a variety of operating conditions and in completing relevant optimisation studies. Moreover, it has undergone further experimental validation, on the basis of over 200 fermentation campaigns carried out over a period of three years (Andrés-Toro et al., 2004).

Trelea at al. (2001) developed a fermentation model based on CO_2 production, using real-time CO_2 concentration data obtained with commercially available sensors (Corrieu et al., 2000). This is deemed an appropriate basis for a fermentation model, as it has been validated to represent a reliable indicator of ethanol and yeast production and sugar consumption (Stassi et al., 1987). Three dynamic models to predict CO_2 production are considered based on varying knowledge of the underlying biochemical phenomena. The first model is a neutral network (black box) and is purely statistical, based on experimental data and computed parameters which are not representative of any physical property. The second (empirical) model is based on a *posteriori* analysis of the form of the experimental profiles recorded: parameter selection and definition occurs after observing the shapes of these curves, however they have little biological significance. Finally, the third (knowledge-based) model is developed in order to represent the true kinetic pathways, producing a complex model formulation which is challenging to validate structurally as well as computationally.

2.2 DYNAMIC MODEL DESCRIPTION

First-principles mathematical modelling for systematic process simulation and optimisation is well established in several (but not all) chemical and material process industries: its importance for ensuring the highest process efficiency and profitability becomes evident when employed in the context of unconventional applications, such as high-temperature multiple rector design (Gerogiorgis et al., 2001; Gerogiorgis and Ydstie, 2005), fossil fuel production (Gerogiorgis et al., 2006), polygeneration (Liu et al., 2007), cyclic dynamics (Akinlabi et al., 2007) and structured products (Angelopoulos et al., 2013; 2014).

The reduced-order kinetic model of beer fermentation by de Andrés-Toro et al. (1998) has been selected for industrial fermentation process simulation for several reasons:

- Published parameters are derived from a very large array of experiments, resulting in a wide temperature range (8–24 ºC) which ensures high fidelity and applicability.

- The model includes all prominent by-products which degrade beer product quality in terms of taste and aroma, rendering the model valuable for assessing performance.
- Predicted profiles indicate the highest fidelity with experimental and pilot-plant data in comparison to other models, due to successful validation against over 200 fermentations.

A description of this kinetic model corresponds to the schematic diagram presented (Fig. 2a).

2.2.1 BIOMASS EVOLUTION

The initial cell culture pitched into the fermenter has a specific composition of active, latent and dead yeast cells, which is defined (de Andrés-Toro et al., 1998) as:

$$0.02 \cdot X_{act}(0) + 0.48 \cdot X_{lag}(0) = X_{dead}(0) = 0.5 \cdot X_{inc} \quad (1)$$

Following their introduction to the system, yeast cells are immediately suspended in the wort, rendering the total suspended cell concentration at any time equal to the sum of all respective cell types:

$$X_{sus}(t) = X_{act}(t) + X_{lag}(t) + X_{dead}(t) \quad (2)$$

During the fermentation lag phase, yeast cells undergo conversion into active cells, which have an enzymatic effect on the sugar substrate:

$$\frac{dX_{lag}}{dt} = -\mu_L(T) \cdot X_{lag}(t) \quad (3)$$

The specific rate of activation (μ_L) is highly sensitive to temperature. During the lag phase, active cells are not considered to grow; their concentration changes due to cell activation:

$$\frac{dX_{act}}{dt} = -\frac{dX_{lag}}{dt}, \qquad t < t_{lag} \quad (4)$$

During the lag phase, cell death is not considered: the suspended dead cell concentration is governed only by the settling rate of cells escaping the suspension toward the tank bottom:

$$\frac{dX_{dead}(t)}{dt} = -\mu_{SD}(T, t) \cdot X_{dead}(t), \qquad t < t_{lag} \quad (5)$$

The dead cell settling rate (μ_{SD}) depends on wort density, which is in turn related to the initial sugar concentration (C_{s_0}):

$$\mu_{SD} = \frac{\mu_{SD_0}(T) \cdot 0.5 \cdot C_{s_0}}{0.5 \cdot C_{s_0} + C_e(t)} \tag{6}$$

The maximum settling rate (μ_{SD_0}) occurs at the beginning of the process, and is also highly to be sensitive to temperature. An Arrhenius equation is used to describe the temperature dependence of all rate parameter expressions within the model, where the constants A and B are estimated on the basis of experimental data at different temperatures (Table 1):

$$\mu_{i_0} = exp\left(A_i + \frac{B_i}{T(t)}\right) \tag{7}$$

Combining Eq. (2) with the aforementioned rate expressions for each cell type produces the overall suspended cell balance for the lag phase:

$$\frac{dX_{sus}(t)}{dt} = -\frac{dX_{dead}(t)}{dt}, \qquad t < t_{lag} \tag{8}$$

Once active cells constitute a significant portion of suspended biomass, the lag phase is completed and the fermentation phase begins. Active cell growth occurs thereafter; suspended cell concentration evolves as a function of both active cell growth and dead cells settling:

$$\frac{dX_{sus}(t)}{dt} = \mu_x(T,t) \cdot X_{act}(t) - \mu_{SD}(T,t) \cdot X_{dead}(t), \qquad t \geq t_{lag} \tag{9}$$

The specific growth rate (μ_x) is a nonlinear function of sugar and ethanol concentrations:

$$\mu_x = \frac{\mu_{x_0}(T) \cdot C_s(t)}{k_x + C_e(t)} \tag{10}$$

The rate at which active cell concentration evolved during the fermentation phase is a combination of active cell growth, active cell death and latent cell activation:

$$\frac{dX_{act}}{dt} = \mu_x(T,t) \cdot X_{act}(t) - \mu_{DT}(T) \cdot X_{act}(t) + \mu_L(T) \cdot X_{lag}(t), \quad t \geq t_{lag} \tag{11}$$

Throughout the fermentation phase, the evolution of latent cells is governed by Eq. (3), however the suspended dead cell ODE must incorporate an additional term to account for the death of active cells:

$$\frac{dX_{dead}}{dt} = -\mu_{SD}(T) \cdot X_{dead}(t) + \mu_{DT}(T) \cdot X_{act}(t), \qquad t \geq t_{lag} \tag{12}$$

The rate of cell death (μ_{DT}) depends on wort temperature, described with an Arrhenius equation (Table 2).

2.2.2 SUGAR CONSUMPTION

The uptake of sugar from wort is proportional to active biomass concentration:

$$\frac{dC_S}{dt} = -\mu_S(T,t) \cdot X_{act}(t) \tag{13}$$

The consumption rate (μ_S) has been assumed to follow Michaelis-Menten kinetics: the maximum rate (μ_{s_0} at $t=0$) corresponds to the maximum sugar concentration which obeys an explicit temperature dependence:

$$\mu_s = \frac{\mu_{s_0}(T) \cdot C_s(t)}{k_s(T) + C_s(t)} \tag{14}$$

2.2.3 ALCOHOL PRODUCTION

Ethanol concentration data shows that its production rate is not constant, so it is necessary to include an inhibition factor (f) in the formulation:

$$\frac{dC_E(t)}{dt} = f(t) \cdot \mu_e(T,t) \cdot X_{act}(t) \tag{15}$$

This factor accounts for the ethanol inhibiting effect in the wort, and is defined along with the specific growth rate (μ_e):

$$f = 1 - \frac{C_e(t)}{0.5 \cdot C_{s_0}} \tag{16}$$

$$\mu_e = \frac{\mu_{e_0}(T) \cdot C_s(t)}{k_e(T) + C_s(t)} \tag{17}$$

2.2.4 BY-PRODUCT PRODUCTION

Ethyl acetate production rate is considered proportional to active cell growth; the stoichiometric factor (Y_{EA}) is an Arrhenius function of system temperature (Table 2):

$$\frac{dC_{EA}(t)}{dt} = Y_{EA}(T) \cdot \mu_x(T,t) \cdot X_{act}(t) \quad (18)$$

The model considers two chemical pathways for diacetyl evolution; the first term accounts for its production rate (proportional to sugar concentration) while the second term represents its conversion rate to other components (proportional to ethanol concentration):

$$\frac{dC_{DY}(t)}{dt} = \mu_{DY} \cdot C_S(t) \cdot X_{act}(t) - \mu_{AB} \cdot C_{DY}(t) \cdot C_E(t) \quad (19)$$

2.2.5 PARAMETER VALUES

Parameter values required in all modified Arrhenius temperature equations defined in Eq. 10 use the ideal gas law constant ($R = 8.314$ J K^{-1} mol^{-1}) and are reported for T in K (Table 1).

Table 1. Experimentally determined Arrhenius constants for Eq. (7).

Parameter Symbol	Description	A_i	B_i
μ_{SD_0}	Maximum dead cell settling rate	33.82	−10033.28
μ_{x_0}	Maximum cell growth rate	108.31	−31934.09
μ_{s_0}	Maximum sugar consumption rate	−41.92	11654.64
μ_{e_0}	Maximum ethanol production rate	3.27	−12667.24
μ_{DT}	Specific cell death rate	130.16	−38313
μ_L	Specific cell activation rate	30.72	−9501.54
$k_e = k_s$	Affinity constant	−119.63	34203.95
Y_{EA}	Ethyl acetate production stoichiometric factor	89.92	−26589

The original model (de Andrés-Toro et al., 1998) describes the specific appearance and disappearance rates of diacetyl (μ_{DY} and μ_{AB} respectively) using second-order temperature polynomials: this description predicts erroneous species profiles, entirely different from those shown in the paper and reported in all experiential studies published. Subsequent papers (Carrillo-Ureta et al., 2001, Xiao et al., 2004) use experimentally determined constants for these growth rates and present profiles in closer agreement with experimental data (Table 3).

Table 2. Experimentally determined diacetyl rates.

Symbol	Parameter Description	Value	Units
μ_{DY}	Diacetyl production rate	$1.27672 \cdot 10^{-7}$	g^{-1} h^{-1} L
μ_{AB}	Diacetyl consumption rate	$1.13864 \cdot 10^{-3}$	g^{-1} h^{-1} L

While investigating the predictive power of the various kinetic models, the present study has discovered that the original de Andrés-Toro kinetic model publication (1998) did not

produce the ethyl acetate profile presented in the paper. This error has been reproduced by numerous authors referencing the model, despite not presenting profiles which follow this mathematical description (Carrillo-Ureta et al., 2001; Xiao et al., 2004). Carrillo-Ureta (1999) defines an ethyl acetate ODE identical to that of de Andrés-Toro (1998):

$$\frac{dC_{EA}(t)}{dt} = Y_{EA}(T) \cdot \frac{dC_S(t)}{dt} = Y_{EA}(T) \cdot \mu_S(T,t) \cdot X_{act}(t) \quad (20)$$

The factor Y_{EA} stoichiometrically correlates sugar consumption to ethyl acetate production. However, inspection of the code presented reveals the simulations are considering ethyl acetate production to be a function of the biomass growth rate (μ_x) rather than sugar consumption rate (μ_S). The later work by the original author (Andrés-Toro et al., 2004) redefines the ODE, confirming that ethyl acetates growth rate is in fact a function of biomass growth rate, as later detailed in Eq. (18) along with the complete model description.

2.3 PUBLISHED OPTIMISATION STUDIES

The de Andrés-Toro (1998) kinetic model typically has been the feature of several optimisation studies, seeking a suitable temperature profile for operation. Several authors have proposed different optimisation strategies with unique objective functions, publishing the fermentation temperature profile they have determined as most favourable.

Carrillo-Ureta et al. (2001) used an evolution algorithm in order to determine such an optimal profile; the procedure is based on the natural selection principal, employing historical simulations to predict new conditions toward achieving greater performance. Their objective function considers the final concentration of ethanol as well as both flavour-degrading species diacetyl and ethyl acetate), and penalises high temperature gradients which are undesirable due to operational adjustment limitations related to cooling jacket maximum capacity and operability. The evolutionary algorithm has successfully generated the same profile maximising the objective function irrespective of the initial profile considered, showing that a global optimum has been reached. However, it highly variable despite the gradient penalty within the objective function, hence impractical for industrial use (Fig. 3a). By averaging the original profile over 40-hour intervals, the authors produced a manipulation protocol which is more suitable for industrial implementation (Fig. 3b). Genetic algorithms constitute a powerful stochastic methodology which is successfully used for multi-objective optimisation of numerous biological processes (Lee et al., 2007; Singh et al., 2009; Taras et al., 2011).

Xiao et al. (2004) also used the de Andrés-Toro model to compute their own optimal temperature profile. The authors developed a stochastic (ant colony system) algorithm to

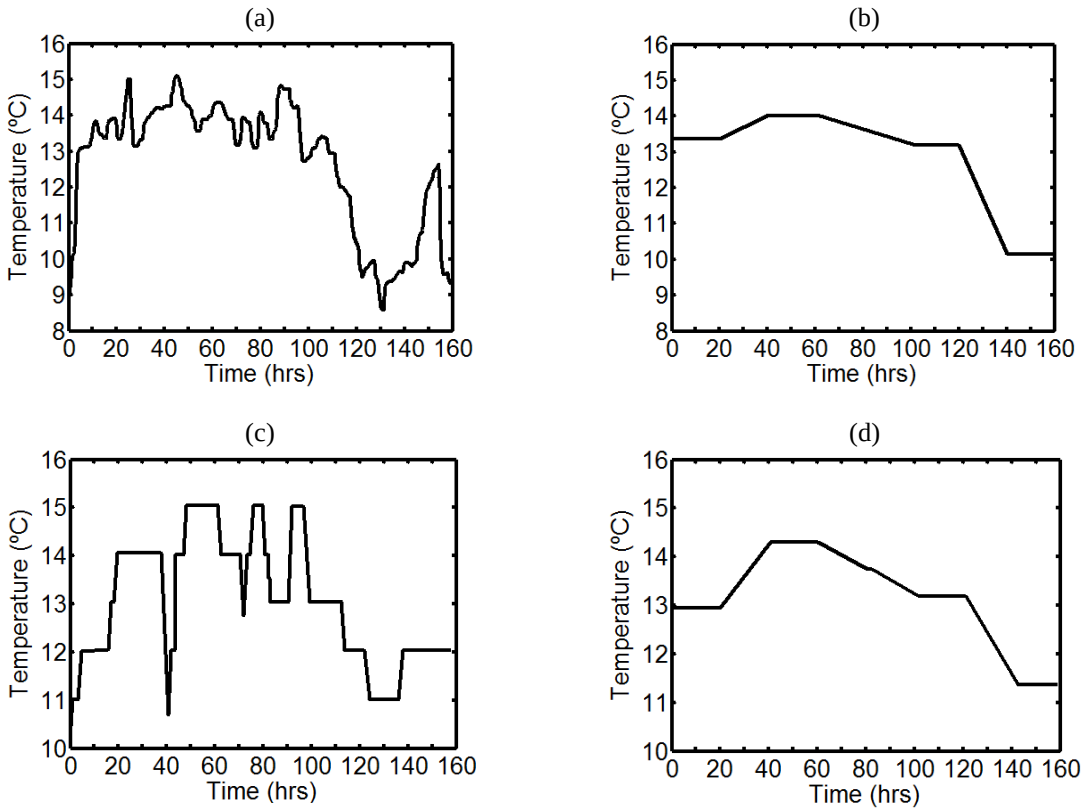

Figure 3. Optimal temperature profiles: Carrillo-Ureta et al.,(2001): (a) as determined, (b) smoothed; Xiao et al., (2004): (c) as determined, (d) smoothed.

arrive at the optimal solution: this powerful heuristic tool can be used to determine the most suitable path through a graph, based on the behaviour of actual ant colonies. The algorithm relies on moving randomly across the domain, determining the value of the objective function continuously while progressing. This data (representing the pheromone which ants leave) gives an indication of how desirable a path decision has been, thus rendering subsequent passes less random and more closely following the most desirable historical routes. The procedure is carried out iteratively until paths through the domain converge on the optimal solution, the equivalent of an ant colony having found the quickest route to a food source. The objective function in this work resembles one used previously (Carrillo-Ureta et al., 2001) but without considering batch time minimisation, as the optimisation procedure requires the target domain, and thus time to simulate fermentation, to be a priori defined. The profile

produced (Fig. 3c) is prohibitively varying for industrial application, so a similar averaging procedure has been used to generate a smoothed form of the optimal manipulation (Fig. 3d).

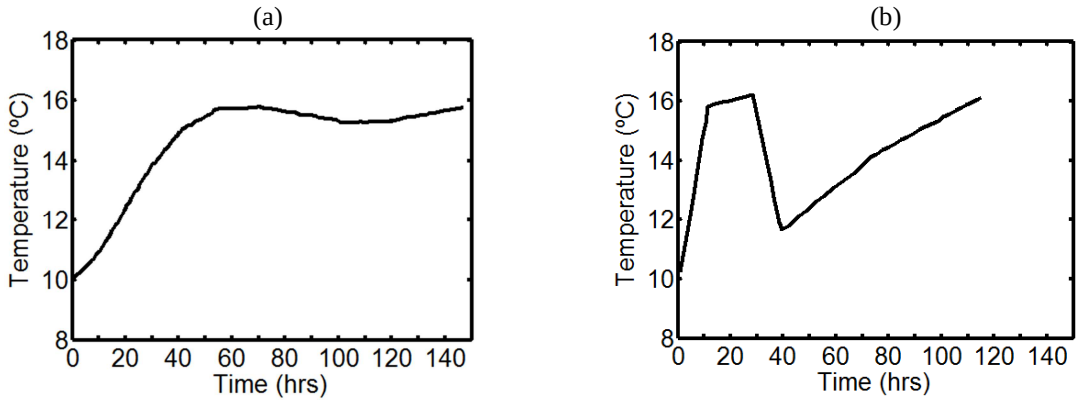

Figure 4. De Andrés-Toro et al. (2004) optimal temperature profiles: (a) improved control, (b) minimum time.

De Andrés-Toro et al. (2004) also performed multi-objective optimisation using the original kinetic model. An evolutionary algorithm (similar to that of Carrillo-Ureta et al., 2001) is used, where each gene can represent a variable time interval between discrete temperature points. The objective function used considers 8 goals: three high-priority targets are treated as system constraints, ensuring ethanol concentration is above (while diacetyl and ethyl acetate concentrations are below) specified levels. The five lower-priority targets consider contamination risk (bacterial formation at high temperature), temperature profile smoothness, batch time as well as instantaneous heat flow and heat flow smoothness. The last two aspects are used to improve process control (prior work has not considered implications of temperature and heat flow profiles on coolant demand). Assigning different weights to the respective targets within the objective function yields different temperature profiles which address unique goals: this strategy can thus achieve (a) improved process control as a result of improved heat smoothness (Fig. 4a), and (b) reduce total batch fermentation time (Fig. 4b).

3. KINETIC MODEL SIMULATIONS

To perform computational simulations of an industrial fermentation process and determine manipulations capable of operational improvements, it is necessary that both the reduced-order kinetic model is suitably descriptive of the process and that the experimentally determined model parameters are appropriately portray the scenario under consideration.

3.1 COMPUTATIONAL IMPLEMENTATION

To compute the dynamic profiles of all chemical species considered in the kinetic model a MATLAB® algorithm has been developed. A function file contains all ODEs (Eqs. 4-22) as well as functions for each temperature-dependent parameter. A script file is used to input all initial conditions as well as the temperature manipulation profile, and the simulation execution follows. The MATLAB® *ode45* function numerically solves the nonlinear dynamic fermentation model along the entire predefined timespan, which must be suitably long to ensure that fermentation is complete. The continuous 250-hour time span is split into 1000 intervals, recording concentration data every 15 minutes, a higher resolution than that used for experimental measurements. An algorithm is built into the function file in order to compute from the input temperature profile the corresponding instantaneous temperature, allowing all model parameters to be recalculated at each iteration.

The assumed biomass and sugar concentrations present in the wort prior to fermentation are given in Table 3 with all other initial species concentrations equal to zero. Uniform initial conditions are considered in all dynamic simulations to ensure that the only factor influencing beer fermentation performance is the temperature manipulation profile employed.

Table 3. Initial conditions for dynamic simulation of beer fermentation.

Symbol	Description	Value	Unit
X_{inc}	Total biomass inoculum concentration (pitching rate)	4	g L^{-1}
C_S	Sugar concentration	130	g L^{-1}

3.2 CODE VALIDATION

To validate the computational code constructed for beer fermentation modelling against de Andrés-Toro's kinetic model (1998), literature temperature profiles have been used as code inputs, allowing comparison of species profiles predicted to those presented by the respective profile authors. The smoothed optimal profiles (Fig. 4b, 4d) from Xiao et al. (2004) and Carrillo-Ureta (2001) have been used, in both cases the code produces profiles with excellent agreement with the literature. Remarkably, Xiao et al. (2004) have omitted ethyl acetate profiles, possibly due to the initial error in describing the respective rate equation, Eq. (20).

3.3 Dynamic Simulation of Industrial Fermentation

The industrial partner (WEST Beer) has provided a unique temperature manipulation for their fermentation process, depicted in Fig. 5a which has been used to simulate concentration profiles of the key chemical species considered in the model, with results shown in Fig. 5(b-d), along with results for an isothermal simulation at 13ºC. Dynamic species concentrations for both prescribed temperature manipulations enables the observation of some significant performance differences. Solid lines in all plots represent the industrial manipulation profile, while dashed lines indicate isothermal operation.

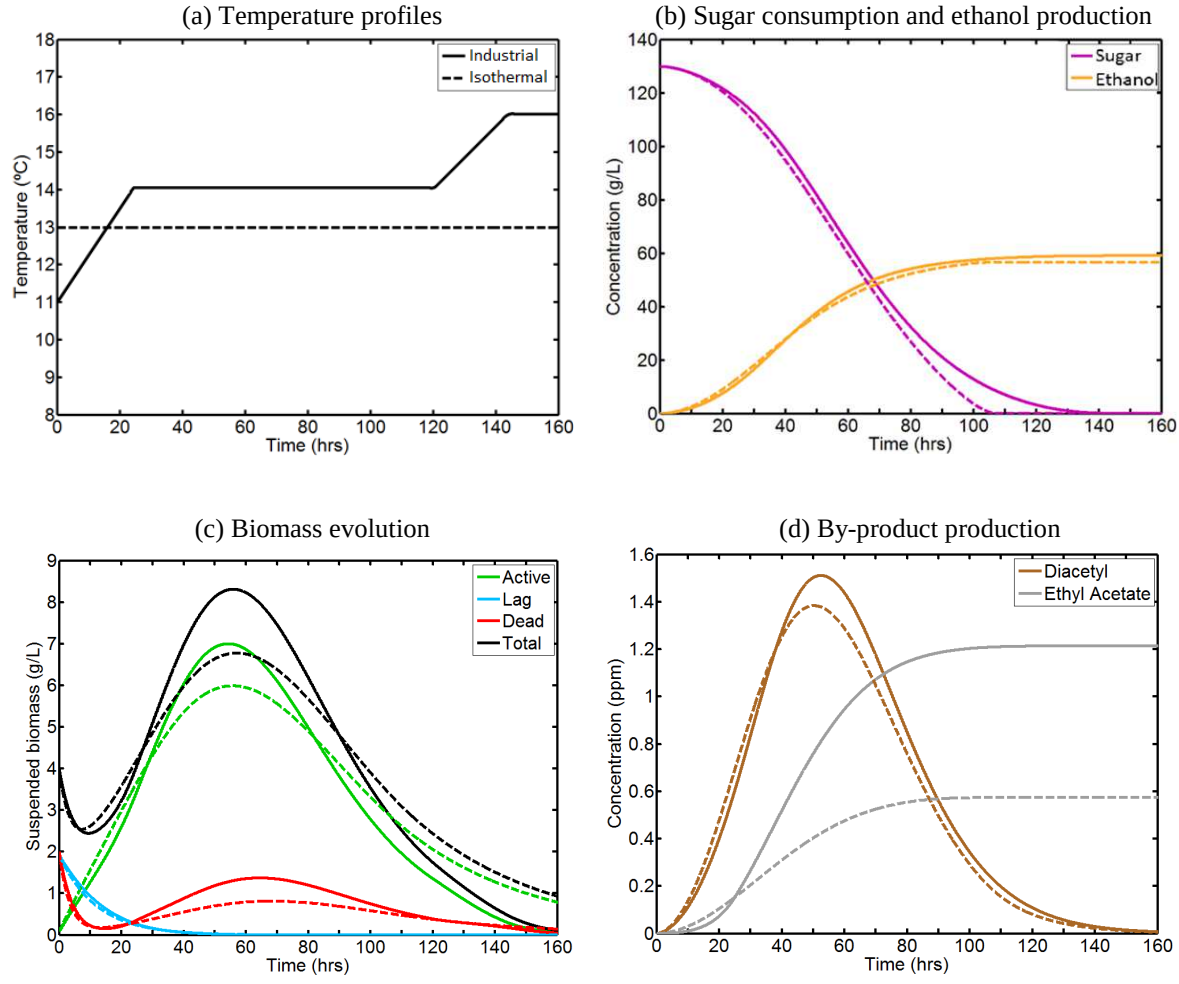

Figure 5. Model species concentration predictions for industrial fermentation operation.

Substrate and product dynamic responses (Fig. 5b) indicate that both temperature profiles promote similar behaviour, with the heightened temperature of the industrial manipulation resulting in greater fermentation efficiency with higher ethanol production. The industrial

profile does however accelerate cell death following the active cell maxima (Fig. 5c) which results in a fermentation taking a greater time to run to completion. The lag phase is shown be of shorter duration in the isothermal case, due to the heightened initial temperature, contributing to the total length of the fermentation process. A significant difference is observed between the predicted dynamic profiles of by-product production (Fig. 5d): diacetyl production is greater for the industrial profile, however so is its consumption resulting in the isothermal case showing over three times greater product concentration. Conversely, the ethyl acetate generated by industrial operation is twice as high as the isothermal case, as a result of the elevated temperature throughout.

3.4 NUMERICAL PROFILE ASSESSMENT

While inspection of species production and consumption plots provides an insight into the performance of the fermentation process, it is more useful to identify precise simulation values which represent adequate performance indicators. Fermentation time is indicative of potential plant profitability: as this is the most time-consuming stage in beer production and the governing factor in the total batch cycle, a viable reduction can have a significant influence on brewery production capacity. Two different methods can be used to analyse fermentation time via the kinetic model, by either monitoring ethanol production or sugar consumption time. Different operational scenarios will result in the production of a range of final ethanol concentrations, so it is incorrect to consider fermentation complete when reaching a target value. Consequently, rather than recording the entire time taken to produce a predefined target concentration, the process shall be simulated for a duration longer than that necessary for fermentation, recording this maximum final ethanol concentration. The time taken to produce 99.5% of this maximum value has thus been considered as the fermentation time required to generate the ethanol concentration, to guard against a 0.5% increase inducing an excessively increased batch duration. While these two values (maximum concentration and batch time) represent fermentation extent and time requirement, they are of little use alone. In case of rapid fermentation where little alcohol is produced with much sugar left unfermented, only the desirable case of high final ethanol concentration in minimal time is to be considered.

A more suitable indicator of fermentation time is arguably sugar consumption, as it encompasses both the extent and the speed of fermentation. Beer will inevitably have some residual unreacted sugar present, so simply recording the time taken to reduce the sugar

concentration to a specified level is a valuable and credible monitor of the process. Care must be taken as this time does not correlate with the amount of ethanol produced, because the later varies for equal levels of sugar consumption under different operational conditions. The most appropriate procedure which has been used in this study is to consider all of: 1) maximum ethanol concentration after a time exceeding that necessary for fermentation, 2) the time to approach this maximum, and 3) the time to consume a specified percentage of the initial sugar concentration. Furthermore, product quality must be considered by recording the concentrations of both aromatic by-products as soon as the process is complete.

Establishing numerical criteria in order to assess the performance of all temperature profiles simulated allows for systematic evaluation and comparison of numerous policies presented in the literature. The maximum potential ethanol concentration is recorded after simulating the process for 160 hours, as this exceeds the time necessary for practical primary fermentation in a lager production process. Ethanol production time is taken as the time to reach 99.5% of this maximum, representing a reliable batch cycle metric. Sugar consumption time is defined as the time taken to reduce concentration to 0.65 g L^{-1} or below, a value representing 0.5% of the initial wort sugar concentration (Table 3) and a typical residual composition after primary fermentation. By-product concentrations are recorded at the point corresponding to the ethanol production time. Dynamic simulation of the fermentation process has been performed using temperature manipulation profiles reported in the literature; results for each of the defined performance indicators are presented below (Table 4). In certain cases, the temperature profile does not facilitate the desired consumption of sugars; in these cases, the sugar concentration at t = 160 hours is presented in parentheses.

Table 4. Fermentation performance of several dynamic temperature manipulation profiles.

Profile: Author (Year)	Figure (this work)	Max. ethanol concentration (g L^{-1})	Ethanol production time (hrs)	Sugar consumption time (hrs)	DA concentration (ppm)	EA concentration (ppm)
Carrillo-Ureta (2001)	Fig. 4b	58.6	106	111	0.14	1.08
Xiao (2004)	Fig. 4d	58.8	116	122	0.10	1.16
de Andrés-Toro (2004)	Fig. 5b	57.8	58	59	1.08	3.16
Isothermal (11 ºC)	-	50.5	115	117	0.20	0.11
Isothermal (13 ºC)	-	56.8	102	105	0.21	0.57
Isothermal (15 ºC)	-	60.6	104	(6.07 g L^{-1})	0.20	2.95
Generic industrial	Fig. 3b	56.1	178	(12.2 g L^{-1})	0.04	1.65
Actual Industrial	Fig. 6a	59.0	121	130	0.06	1.16

Table 4 indicates that the generic industrial temperature manipulation profile reported in literature (Fig. 3b) does not ensure an effective fermentation: not consuming an adequate amount of sugars from the wort and producing a large amount of ethyl acetate, it is representative of established industrial practice but it does not appear to be optimal.

The profile presented by the original author (de Andrés-Toro, 2004) indeed produces very short fermentation times in line with its design goal, but due to the significant aromatic compound production it is not suitable for industrial use. Further optimisation studies based on this model have produced promising results (Carrillo-Ureta et al., 2001; Xiao et al., 2004). The advantages in each study appear in different areas, depending on the respective objective function, highlighting that is extremely difficult to quantitatively prescribe the relative importance of different variables in a real biochemical process to represent the objective function with a single mathematical expression.

When considering the three isothermal dynamic simulations performed, one expects that a higher temperature leads to increased ethanol production and reduced fermentation time, coupled with increased by-product production, which is indeed observed (Table 4). What is not evident, however, is that residual sugar concentration actually increases with fermentation temperature, despite final ethanol concentration increasing: this is a result of the conversion efficiency improving, while the higher rate of yeast cell death reduces sugar consumption.

Comparing the actual industrial manipulation (WEST) to the other profiles simulated reveals that the industrial protocol produces a comparatively high ethanol but a very low diacetyl concentration. Processing time is of the longest of all profiles simulated, indicating there is strong incentive for optimisation. There is also scope for reducing the moderately high ethyl acetate concentration (higher in the industrial case compared to several simulated alternatives) and probably above the threshold for undesirable flavour contribution. These results clearly indicate that the choice of imposed temperature profile which a brewery elects to implement has an extremely strong influence on all aspects of beer fermentation performance, so it must be addressed by systematic modelling and process optimisation.

3.5 IMPLICATIONS OF SMOOTHING

Published temperature profiles from optimisation studies are computed by minimising the respective objective function, which often includes a term which penalises abrupt temperature changes, because such rapid manipulations are very difficult to accurately implement in a

biochemical process. Computed manipulation profiles are often still impractical, so it is necessary to smooth the profile toward facilitating industrial implementation (Fig. 6a).

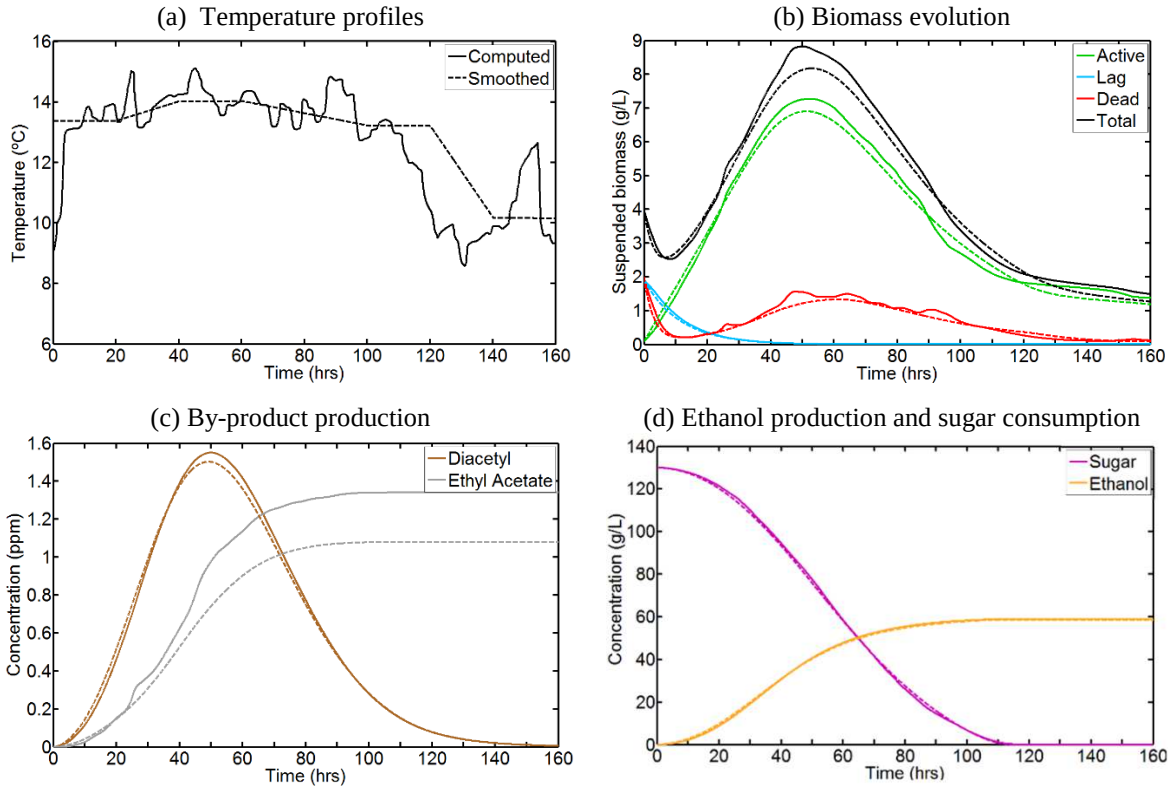

Figure 6. Effect of smoothing on fermentation: (a) profiles from Carrillo-Ureta et al. (2001), (b)-(d): this work.

The literature cited does not analyse the implications of this secondary smoothing procedure on process performance: smoothing is generally carried out by averaging the computed temperature profile over large time intervals. The non-implementable computed profiles have simulated within this study in order to assess the impact of smoothing on fermentation performance: Figs. 6-7 illustrate the resulting variation of dynamic species concentration profiles, and key result parameters are summarised in Table 5.

Table 5. Performance implications of profile smoothing.

Profile author	Figure (this work)	Temperature input profile	Max. ethanol concentration (g L^{-1})	Ethanol production time (hrs)	Sugar consumption time (hrs)	DA concentration (ppm)	EA concentration (ppm)
Carrillo-Ureta et al. (2001)	Fig. 6	computed	59.0	106	112	0.13	1.35
		smoothed	58.6	106	111	0.14	1.08
Xiao et al. (2004)	Fig. 7	computed	58.5	125	136	0.05	1.35
		smoothed	58.8	116	122	0.10	1.16

Manipulation profiles are simulated exactly as published by the respective authors: in each case solid lines depict operation of the optimal profile, while dashed lines are the authors' own smoothed result. While Figs. 6-7 show that species concentration evolution is influenced by smoothing, Table 5 data indicates that the effect of smoothing on process performance is minimal: in general, smoothed model predictions implying improved plant performance.

Carrillo-Ureta's manipulation (2001) has led to a small penalty in maximum ethanol production: depending on the fermentation time metric, an increase in batch time can also be observed. A small increase (0.01 ppm) in final diacetyl concentration is accompanied by a large (20%) reduction in ethyl acetate concentration after profile smoothing. Xiao et al. (2004) have obtained clear improvements in all variables after smoothing, producing more ethanol in a shorter time: while diacetyl production has doubled, it is still low relative to other manipulations simulated (Table 4). This is particularly surprising, given that the computed profile must have produced an objective function with a more desirable value than that of the smoothed scenario, otherwise their algorithm would have already arrived at that optimum.

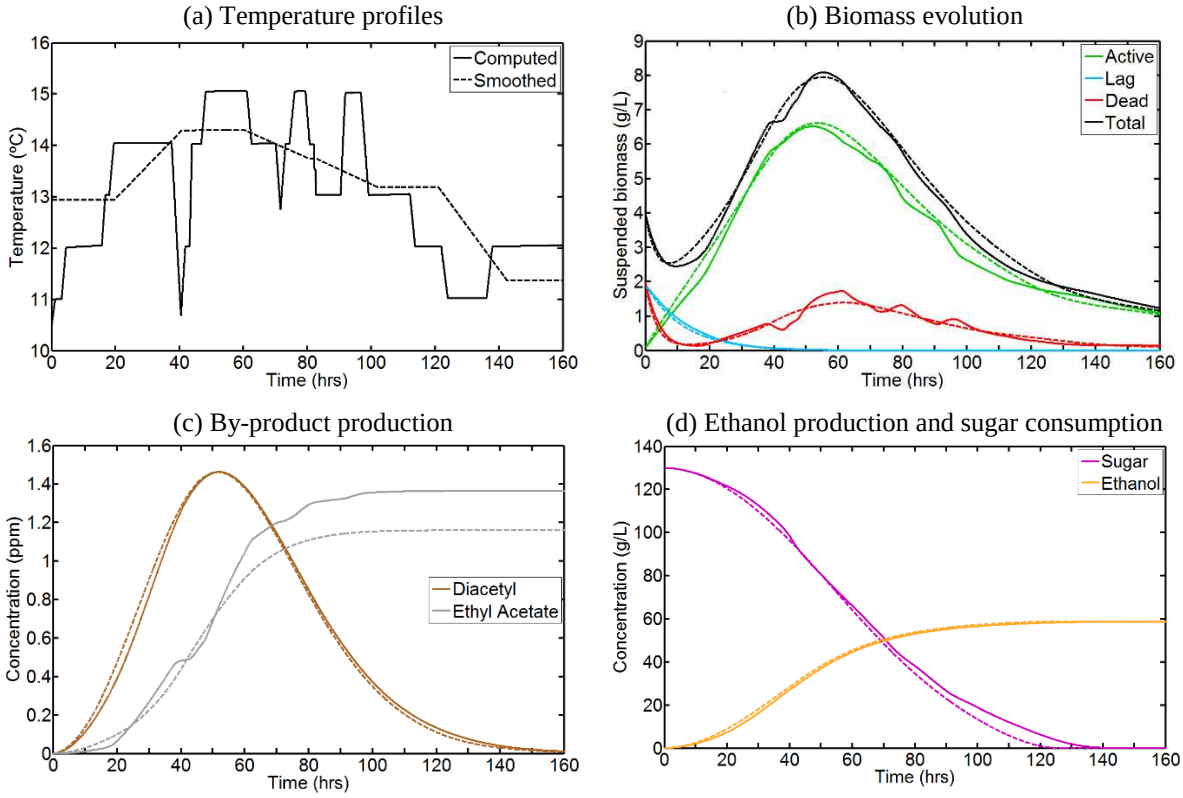

Figure 7. Effect of smoothing on fermentation: (a) profiles from Xiao et al. (2001), (b)-(d): this work.

This suggests component weights in the authors' objective function may not have accurately represented the importance of all different output variables, thus ascribing more importance to reducing diacetyl concentration than to processing time or ethanol production. Furthermore, it is possible that the authors' objective function considered by-product concentrations at the end of the simulation, rather than at the point when fermentation is complete which is of more value for assessment of fermentation performance.

4. PROCESS OPTIMISATION BY DYNAMIC SIMULATION

A comprehensive review of published fermentation literature yields numerous temperature manipulation profiles which are presented as optimal: these have been evaluated by dynamic simulation (Table 5), indicating that while many of them have relative merits, it is extremely challenging to quantify which performs best, given the competing targets for process improvement. A more rigorous exploration of potential dynamic temperature manipulations has been performed in this study toward determining if and how the WEST Beer process can benefit from modification of the current temperature manipulation profile. Enhancing profitability is highly important and only achievable if a novel operating procedure can be demonstrated to reduce batch cycle time, thus allowing plant throughput to be increased.

4.1 METHODOLOGY

To assess the potential for process improvements in current plant operation at WEST Brewery, an algorithm has been developed to rapidly generate plausible temperature manipulations which adhere to realistic operability constraints at a suitable level of temporal domain discretisation. The systematic stochastic investigation of potential improvements relies on generating a vast number of potentially suitable temperature profiles and simulating fermentation for each dynamic manipulation. Plotting the entire set of different performance indicators obtained from each dynamic simulation along with those known from the current industrial manipulation can thereafter reveal the entire performance envelope towards pinpointing which precise process improvements are feasible.

To generate new manipulations, the temperature domain must be rigorously discretised. The domain limits have been defined by Eqs. (21)-(22): the time span is such that any profile producing reasonable performance will be run to completion, while avoiding unreasonable computational load for all profiles which imply a prohibitively long batch time. The lower

temperature limit excludes scenarios in which the system lacks enough energy to promote cell growth; the upper limit ensures bacteria which are present above this temperature cannot thrive, while also preventing the temperature from reaching a level at which undesirably high by-product concentrations are known to be produced.

$$0 < t < 160 \text{ (hours)} \tag{21}$$

$$9 < T < 16 \text{ (ºC)} \tag{22}$$

An extremely large number of paths within this finite domain exists, so discretisation is necessary in order to obtain a manageable finite set. Temperature control of industrial fermentation vessels is extremely challenging, given the complex flow patterns in fermentors: consequently, attempting to manipulate the temperature to a finer level 1 ºC is not practical. The temperature range considered has thus been discretised per degree, with 8 values considered in total, between which the temperature is taken to vary linearly. For a manipulation profile to be implementable, the temperature must not change abruptly with time, to avoid imposing unrealistic demands on the cooling system. To accommodate this, the fermentation time span is broken down into 20-hour intervals, so 9 values are considered along the time axis, thus producing temperature profiles which all consist of 8 linear segments. This discretised grid will produce 9^8 total unique paths, a value too vast for exhaustive numerical dynamic simulation. Many of these paths are evidently not industrially implementable, so it is necessary to select and simulate only technically promising cases.

Constraints must be applied in order to reduce the number of paths, removing those which evidently produce poor performance and induce an unnecessary computational burden. An investigation has been performed in order to identify appropriate profile constraints, which must reduce the total number of profiles (paths) to a manageable level, selecting those likely to produce good performance while also allowing a reasonable range of different paths to be considered so that the effect of various operating conditions can be assessed. A set of different rules for profile constraints has been developed conceptually. Rule A states that temperature may only increase to any level within the domain limits or remain constant when progressing to the nest discretised point in time.

Rule A: $$T(t_{n+1}) \geq T(t_n) \tag{23}$$

In rules B and C, the temperature is allowed to either remain constant, increase or decrease when progressing to the next time point. Rules B uses X = 1 ºC and rule C considers X = 2 ºC to limit the temperature change between each interval; e.g. in the latter a variation of 0, 1 and 2 ºC in both directions is considered at every time step:

Rules B and C: $$T(t_n) - X \;\leq\; T(t_{n+1}) \;\leq\; T(t_n) + X \qquad (24)$$

One more set of rules have been considered, in which the constraint is split in time such that the temperature may only increase up to X degrees for the first half of the process, and then only decrease up to X degrees between successive time steps for the second half of the fermentation. Rule D selects X = 1 ºC, rules E imposes X = 1 ºC and F considers X = 3 ºC. This early increase and later decrease represents the form generally employed in fermentation.

Rules D, E, F: $$T(t_n) \;\leq\; T(t_{n+1}) \;\leq\; T(t_n) + X, \quad \text{for } t < \frac{t_{max}}{2} \qquad (25)$$

$$T(t_n) - X \;\leq\; T(t_{n+1}) \;\leq\; T(t_n), \quad \text{for } t \geq \frac{t_{max}}{2} \qquad (26)$$

The number of paths generated when following each of these constraints is listed in Table 10, for increasing levels of time domain discretisation. Rule A produces a low number of paths, but limiting temperature evolution such that it can only increase is highly restrictive because cases which include a later decrease in temperature (as often shown in literature) are excluded. Rules B and C are much less restrictive, as temperature increase or decrease at any point is permitted. However, the number of paths produced increases explosively as the allowable ΔT between time points increases. This is clear in Table 1, where increasing the allowable temperature variability from 1 ºC (B) to 2 ºC (C) drastically influences the number of profiles, with the gap growing dramatically as the permitted temperature change is further increased. Rules D, E and F show a much less severe impact on the number of paths when

Table 10. Number of unique profiles for various constraint rules and increasing time domain resolution.

Rule	X (ºC)	Eq. number(s)	Number of time points:	4	5	6	7	9
			t_{step} (hrs):	53.33	40	32	26.67	20
A		(25)		120	330	792	$1.7\cdot10^3$	$6.4\cdot10^3$
B	1	(26)	**Number**	62	176	502	$1.4\cdot10^3$	$1.2\cdot10^4$
C	2	(26)	**of unique**	512	$4.1\cdot10^3$	$3.3\cdot10^4$	$2.6\cdot10^5$	$1.7\cdot10^8$
D	1	(27), (28)	**manipulation**	29	55	106	201	730
E	2	(27), (28)	**profiles:**	59	157	434	$1.1\cdot10^3$	$7.8\cdot10^3$
F	3	(27), (28)		94	305	$1.1\cdot10^3$	$3.2\cdot10^3$	$2.7\cdot10^4$

increasing ΔT, while still including typical fermentation cases, and has been found to be the most suitable of all novel constraints we have developed. To allow a greater range of potentially suitable paths to be simulated, Eqs. (25-26) are modified to remove the permitted temperature step limit, allowing any level of temperature variation between time points while still following the same multi-region constraint rule, as seen in Eqs. (27-28). This double constraint states that all levels of temperature increase within the domain limits are considered for every time step before the midpoint, and all levels of decrease are considered for every step after the midpoint. Accordingly, a large set of potentially applicable profiles has been obtained for the fermentation process.

Applied constraint:

$$T(t_{n+1}) \geq T(t_n), \quad \text{for } t < \frac{t_{max}}{2} \tag{27}$$

$$T(t_n) \geq T(t_{n+1}), \quad \text{for } t \geq \frac{t_{max}}{2} \tag{28}$$

4.2 SIMULATION RESULTS

The temperature and time limits, discretisation level and constraints considered in the present study produce 175,252 unique temperature profiles. Simulating dynamic species evolution for the entire set of manipulations requires 3 hour of total CPU time. Key performance indicator data from all dynamic simulations are plotted and compared to the actual industrial operating profile point (WEST) represented by the circular blue marker on the scatter plots (Figs. 8-9).

Fig. 8a illustrates all final concentrations of ethanol, diacetyl and ethyl acetate after fermentation for 160 hours, for every single scenario simulated, providing a three-dimensional indicator of product quality. Fig. 8b presents a measure of process performance by correlating fermentation efficiency (measured by maximum ethanol production) and fermentation time (measured by the time to produce 99.5% of that value). Here the desirable region is the upper left corner of the figure, representing maximum ethanol concentration in minimum time. Fig. 8(c-d) similarly show produced aromatic compound concentrations against fermentation time, which is now measured by the time to almost entirely consume the initial wort sugar concentration. While measuring fermentation time by sugar consumption and ethanol production do yield marginally different times, their strong correlation renders either of the two as a reliable indicator of process performance, providing ethanol production and sugar consumption are both adequately high. Using sugar consumption as an indicator

removes cases where undesirably high residual sugar concentration remains in the product, which consequently do not feature in Fig. 8(c-d) or Fig. 9.

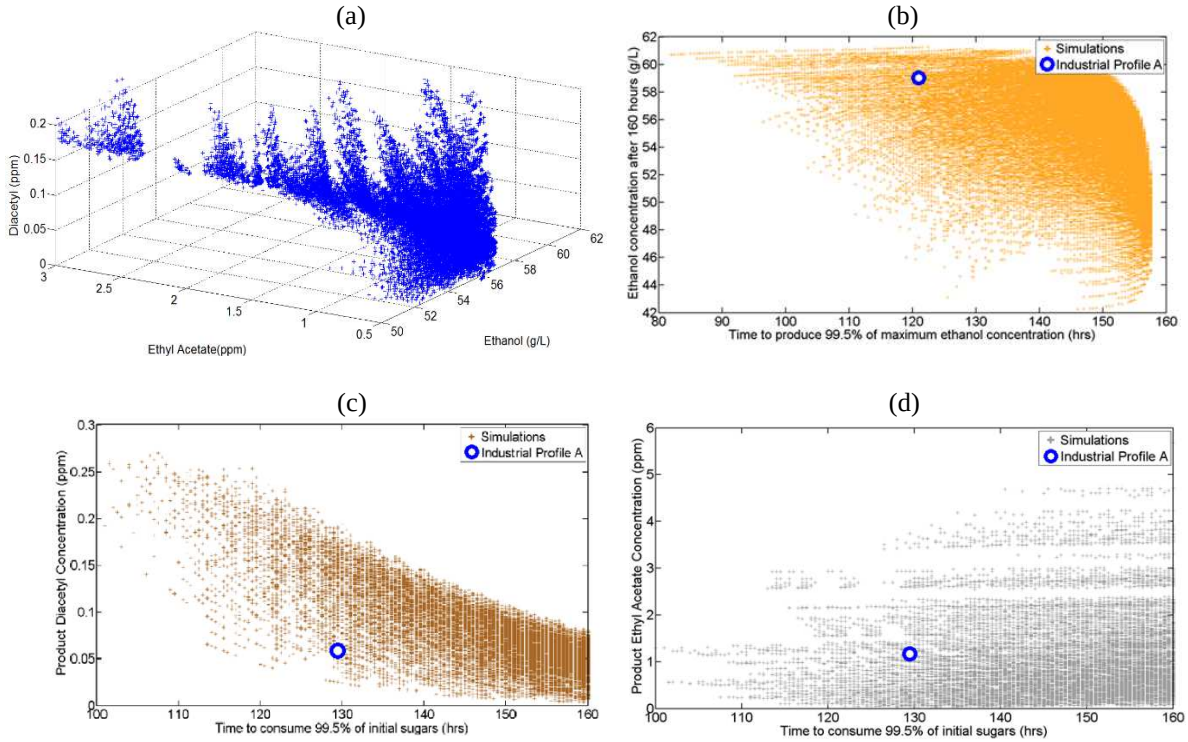

Figure 8. (a) Attainable product envelope; Concentration of (b) ethanol, (c) diacetyl, (d) ethyl acetate vs time.

The process lag phase length is also considered for each simulation in order to determine if it has a strong effect on the total batch time. Thus, Fig. 9a presents the length of the lag phase vs. batch time, while Fig. 9b shows the effect of the lag phase length on the maximum active cell concentration observed within the yeast culture.

Figs. 9(c-d) present the active cell population against batch time: Fig. 9c compares fermentation time to maximum active cell population, while Fig. 9d considers the final active yeast cell concentration after fermentation is complete: the latter is of high industrial interest, as it is desirable to recover the yeast toward using it in subsequent fermentation batches.

All fermentation performance indicators suggest that the WEST Beer operational profile (Fig. 5) has reasonably high performance, better than a large portion of the simulated alternatives. It is also evident there is significant potential to improve any single variable, however often not without compromising on another target parameter. Thus, Fig. 8a shows the relationship between final product concentrations: it can be seen that the greatest ethanol

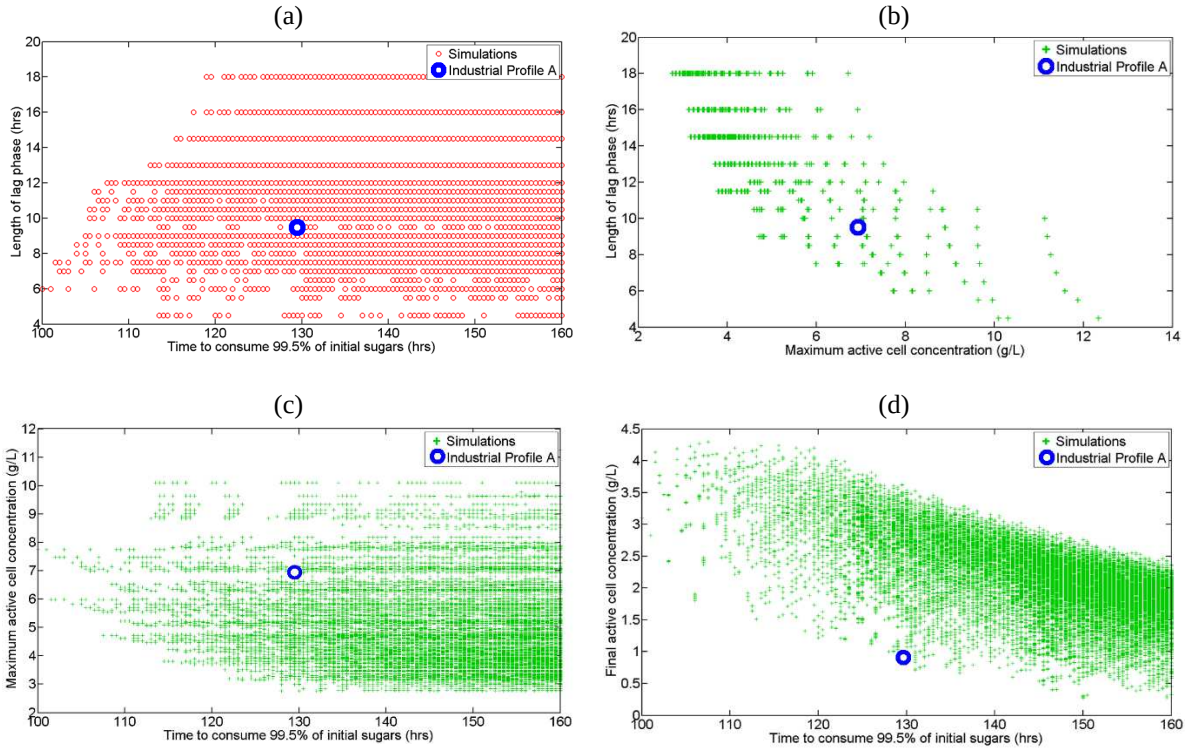

Figure 9. Fermentation performance for all simulations; Lag phase length vs. (a) Batch time, (b) Active cell concentration; Fermentation time vs. (c) Maximum active cell concentration, (d) Final cell concentration.

production also corresponds to the highest production of aromatic by-products, well exceeding acceptable levels. It also indicates that a small sacrifice in final ethanol concentration can lead to large reductions in the concentrations of aromatic compounds present. Moreover, Fig. 8b shows that it is possible to both increase ethanol production and reduce processing time relative to the industrial manipulation (upper left quadrant data points). However, the implications on all other design variables must be considered; the most desirable simulation according to Fig. 8b is the upper leftmost point on the graph, which corresponds to isothermal operation at $T = T_{max}$, but also to very high by-product production and sugars remaining unconsumed. It is more beneficial to retain or marginally reduce the current ethanol production in order to reduce batch time while not impairing product quality.

Furthermore, Fig. 8c illustrates that a reduction in batch time is correlated with an increase in diacetyl in the beer product. The current industrial plant manipulation is producing a low ethyl acetate concentration given the batch time (t = 130 hours), close to the Pareto front of this plot, which follows the minimum concentration boundary for any fermentation time. Diacetyl concentration is the most challenging variable to reduce without suffering a

detrimental effect on other process parameters. Because it is well below the levels produced by most fermentations, it is possible to allow dicatyl concentration to increase within acceptable limits in order to achieve a process improvement in terms of batch cycle time.

Conversely, Fig. 8d shows that such a high level of a correlation between ethyl acetate concentration production and batch time does not exist. Simulation data points are spread out widely, however it is clear that longer batch times can coincide with higher aromatic compound levels, while shortest batch times correspond to the lowest concentrations. The current industrial manipulation produces approximately the average ethyl acetate concentration for all fermentations of this duration.

No apparent trend between the length of the lag phase and the total fermentation time is observed (Fig. 9a). The industrial manipulation corresponds to the average lag phase duration ($t = 130$ hours) this batch duration. The lag phase duration does influence the maximum concentration of active yeast cells which are produced (Fig. 9b): a shorter duration for this lag phase leads to an increased maximum cell concentration.

Also, Fig. 9c reveals that the maximum cell concentration is not closely related to the batch fermentation time, highlighting that this is not an essential parameter for evaluating process performance. The average concentration of active cells is of higher importance, given that a short-lived high maximum does not influence fermentation rate for a long period of time. It is desirable to ensure there is an active cell population when fermentation is complete: Fig. 9d illustrates that while the points are highly spread, the overall trend indicates that rapid fermentations facilitate a higher concentration of active cells at the end of the process. This is extremely significant in case of successfully reducing batch time, because material costs for fresh yeast can be reduced in addition to improving plant throughput.

Simulation results have been analysed to evaluate which cases reduce fermentation time with acceptable effect on product quality. The time for sugar consumption of the preferable industrial manipulation (case A) is 130 hours (Table 5). A 10-hour reduction of fermentation time would have a significant impact on brewery production capacity, so all simulated profiles which produce a batch time under 120 hours must be considered as potentially viable process improvements. Hence, of the profiles simulated, 2759 take 120 hours or less to consume 99.5% of the initial sugars. Many of these differ only after fermentation completion (120 hours), so only 826 potentially suitable profiles can improve the first 120-hour period.

Table 6. Proposed fermentation process improvements.

Parameter	Units	Existing manipulation	Operational improvements (Figure 10)		
			A	B	C
Fermentation time	hrs	129.5	119.5	115.0	119.5
Ethanol concentration	g L^{-1}	59.0	58.9	58.0	58.9
EA concentration	ppm	1.16	1.19	0.99	1.28
DY concentration	ppm	0.06	0.10	0.16	0.09

Three promising process improvement cases are highlighted in Table 6, with the corresponding profiles illustrated in Fig. 10. A considerable batch time reduction is demonstrated in each case, with minimal impact on product quality. Options A and C show similar performance, a 10-hour reduction in fermentation time, with a small (0.1 g L^{-1}) reduction in ethanol produced and a marginal increase in both aromatic compound concentrations. Option B is more preferable if a more significant decrease in ethanol concentration is permitted: a decrease of 1 g L^{-1} can reduce batch time by 15 hours, while also reducing the product ethyl acetate concentration by over 15%. Diacetyl concentration is also increased, however it remains comparatively low compared to other manipulations considered (Table 4). Depending on a brewer's particular product targets, numerous dynamic simulations performed in this study represent clear and measurable process improvements, which can be attained by tolerating small sacrifices in areas considered as process targets of lower priority.

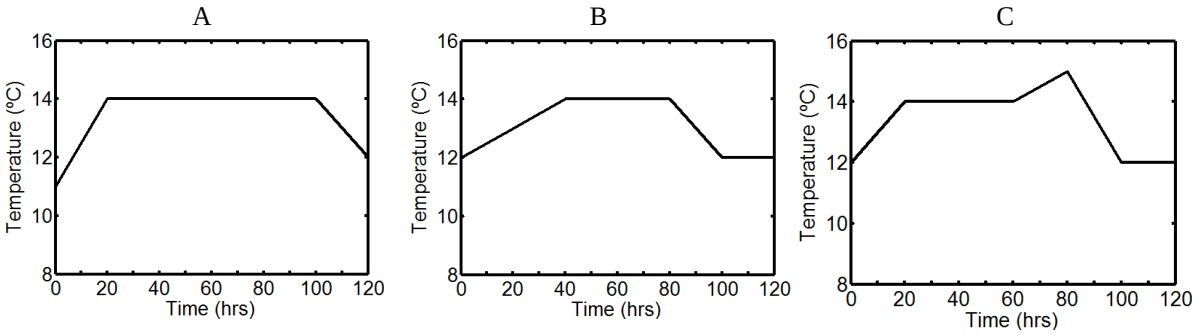

Figure 10. Dynamic temperature manipulation profiles producing clear and measurable process improvements.

4.3 Optimal Temperature Profile Determination

The attainable envelope of product final concentrations (Fig. 8) compiled from the entire data set of simulation results clearly illustrates that numerous plausible manipulations promise superior performance (hence process improvements) over current industrial practice. The

precise determination of the most suitable and advantageous temperature manipulations is hence the next essential step for achieving the best feasible performance (optimal operation). Therefore, two computational procedures have been performed. First, Simulated Annealing (SA) has been implemented so as to determine the optimal temperature manipulation profile in a rapid and efficient manner. Secondly, the performance of each of the 175,000 profiles has been quantified for a range of objective function weights by exhaustive evaluation, in order to validate stochastic optimisation (SA) optimal results, as well as investigate the sensitivity of optima with respect to the arbitrary objective function component weight value allocations.

4.3.1 SIMULATED ANNEALING (SA)

Simulated Annealing (SA) is a valuable approach for approximating a global optimum (Kirkpatrick et al., 1983), requiring significantly less CPU time compared to exhaustive techniques. The metaheuristic for approximate global optimization is applicable to the large search space here, and has been applied to biochemical network processes for parameter estimation previously (Gonzalez et al., 2007). The computational procedure is analogous to the thermal annealing of solids, in which the material is heated and then cooled slowly, allowing atoms to reach a minimal energy state. In simulated (much like in material thermal) annealing, the current candidate solution (system state) may move to another of worse objective function value (akin to a higher energy state), particularly in the early stages of the process. This occurs so that early local minima or maxima can be escaped in the search for the globally optimal solution: as the SA temperature is gradually reduced, the corresponding probability of accepting a worse solution is reduced.

An objective (cost) function is essential to define in order to quantify and compare the performance of fermentation temperature profiles: in principle, it can account for final product concentrations (ethanol, diacetyl and ethyl acetate) and batch time as terminal payoffs, while energy consumption is not considered as a running payoff, in accordance to most previous studies and the model (de Andrés-Toro et al., 1998) employed. The objective function we have formulated only considers final ethanol concentration maximisation and batch time minimisation, and is given by Eq. (29): therein, W_E and W_t are the respective weights of the two components, $\widetilde{\left(\frac{1}{t}\right)}$ is the inverse batch time (normalised by division with the maximum value recorded) and $\widetilde{C_E}$ is the ethanol concentration (normalised in the same

way). In doing so the normalised ethanol concentration, $\widetilde{C_E}$ ranges from 0.68 when $C_E = 42$ g L^{-1} to 1 when $C_E = 61.3$ g L^{-1}, similarly the normalised inverse batch time, $\left(\widetilde{\frac{1}{t}}\right)$, ranges from 0.62 to 1 when t is 99 hrs and 160 hrs respectively. By-product species (diacetyl and ethyl acetate) final concentrations are considered as constraints, since they must be kept below threshold values in the final product, and are given in Eqs. (30-31); further reductions below these limits are welcome but not essential, as they do not induce any discernible effect on flavour (resulting product quality improvements cannot be quantified).

$$J_{MAX} = W_E \cdot \widetilde{C_E} + W_t \cdot \left(\widetilde{\frac{1}{t}}\right) \tag{29}$$

$$s.t. \quad (C_{EA})_{t=t_{final}} \leq 2 \text{ ppm} \tag{30}$$

$$(C_{DY})_{t=t_{final}} \leq 0.1 \text{ ppm} \tag{31}$$

A novel SA algorithm has been developed, based on published MATLAB® code (Optimization Techniques in Engineering, 2015). Firstly, the data set produced via exhaustive simulation is compared to the tolerable by-product limits, Eqs. (30-31), and all cases in which the latter are exceeded are removed (feasible region identification). Secondly, an ethanol concentration is initially assumed, and the corresponding production (batch) time is retrieved: the objective function value corresponding to the respective temperature profile can then be computed using Eq. (29). The SA algorithm then follows the flow diagram given in Fig. 11.

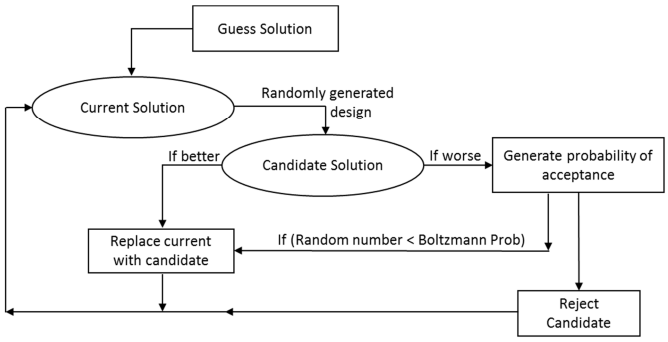

Figure 11. Simulated annealing flow diagram (Optimization Techniques in Engineering, 2015).

A new potential ethanol concentration is generated by stepping randomly from the current value. The corresponding batch time is recorded and the objective function value is computed

again: if the latter shows improvement, it replaces the current solution. If the solution is worse, it may still replace the existing solution if a randomly generated number is less than the Boltzmann probability, Eq. (32) where ΔE is the energy displacement (difference in objective function values for successive iterations), k_b is the is the Boltzmann constant and T is the SA temperature (not to be confused with fermentation temperature):

$$P = \exp(\frac{-\Delta E}{k_b T}) \tag{32}$$

This procedure has been performed for a wide range of objective function component weights (Eq. 29), for several starting points (initial guesses): the optimal point determined is independent of the starting point selected, provided that a suitable cooling rate is used. The number of iterations required and the appropriate starting SA temperature depend on the accuracy of the initial guess. A wide variation of component weights have been used, but only three cases are illustrated (Fig. 12): for each of them, three different starting points (A, B, C) are considered and all three SA trajectories are clearly shown to converge to the same optimal point (which depends on weight allocation), albeit at quite variable performance (iterations). The figure depicts the entire set of simulations results as to allow the SA trajectories to be readily visualised, however the data is not an inherent part of the procedure.

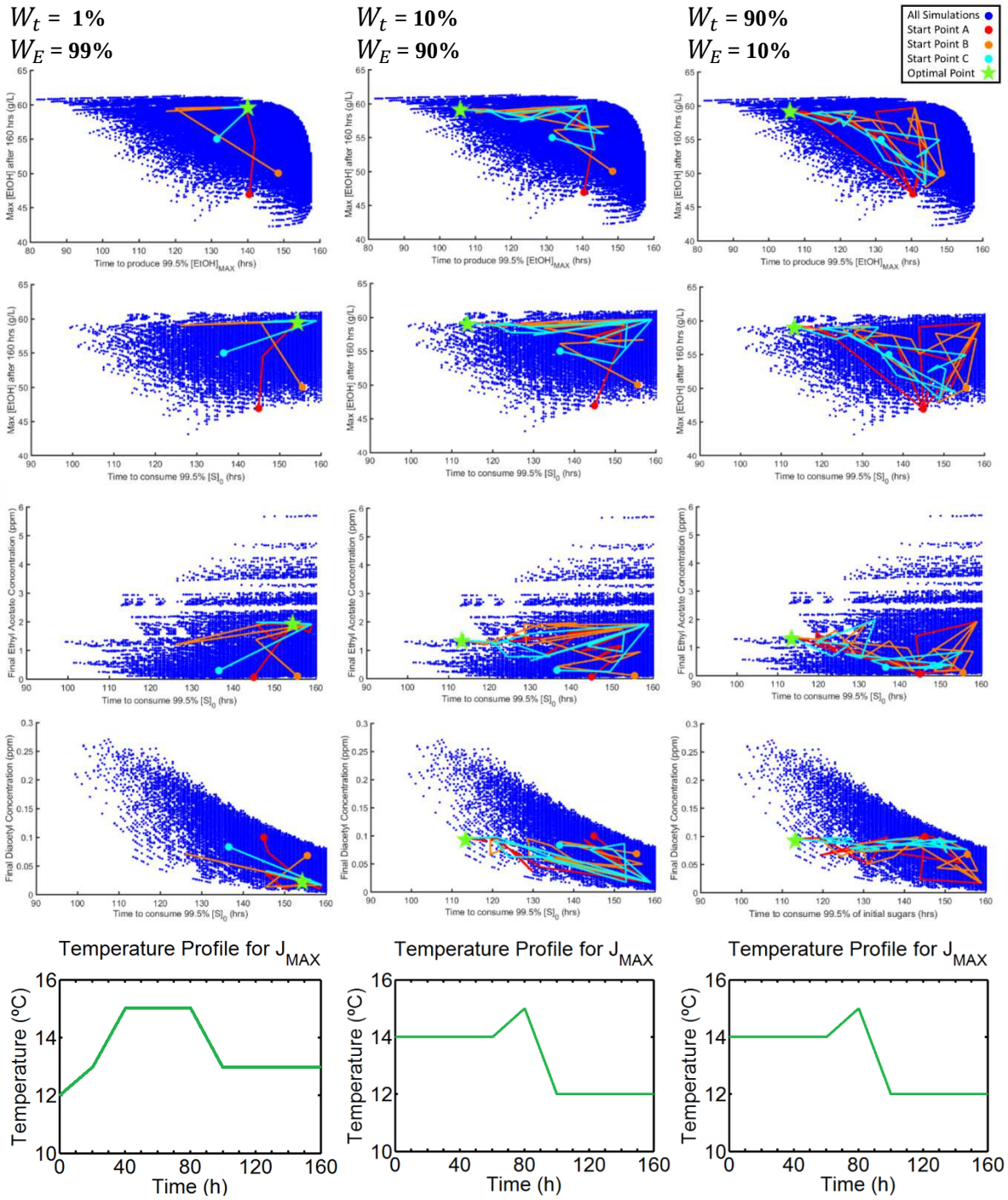

Figure 12. Exhaustive optimisation results for varying J-function component weights.

Furthermore, a remarkable observation is that (while dependent on weight allocation for W_t < 10%), the optimal temperature profile remains identical (and independent of weight allocation) for all cases where W_t > 10%; this trend is significant, because it indicates that the optimal manipulation displays almost no sensitivity to the arbitrary balance of objective

function terms. A minimal reduction of ethanol concentration (Fig. 12, first column) can therefore facilitate a considerable batch time reduction, while also ensuring that Eqs. (30-31) constraints are satisfied. The temperature profile presented (Fig. 12, second and third columns) can thus be conclusively determined as the optimal result for the fermentation process considered, excluding the unrealistic case of extreme (and virtually exclusive) importance of ethanol concentration only (W_E > 10%), in which batch duration is disregarded (W_t < 10%).

A larger number of SA iterations are required when the initial point lies far from the optimal result; also, a higher initial SA temperature is required in these cases so that local maxima can be overcome. In the first case (W_t = 99%, W_E = 1%), the solution lies closer to the starting points, so a lower initial SA temperature and fewer iterations were required. Conversely, the other two weight allocation cases required a higher initial temperature, in order to prevent convergence entrapment in a local minimum and attain the global solution. Fig. 12 (second and third columns) indicates that the SA algorithm passed through the point corresponding to optimal operation in the first case (W_t = 99%, W_E = 1%), as the latter constitutes a local (but not global) maximum for the other two cases. Table 7 shows the required parameters to consistently reach the optimal solution for any starting point in each case. Objective function values and convergence speed are illustrated in Fig.13 for the second case (W_t = 90%, W_E = 10%). CPU time reported corresponds to MATLAB 2013a/Windows 7 64GB running on an Intel Core i7-4700MQ @2.40 GHz with 16 GB installed RAM.

Table 7. Simulated annealing parameters required for solution convergence.

Eq. (29) weights	$T_{initial}$	$P_{initial}$	T_{final}	P_{final}	Iterations	Simulations	CPU time	J_{MAX}
W_t = 99%, W_E = 1%	0.621	0.2	0.1087	0.0001	10	103	586 s	0.97
W_t = 90%, W_E = 10%	9.491	0.9	0.1087	0.0001	30	364	1571 s	0.92
W_t = 10%, W_E = 90%	9.491	0.9	0.1087	0.0001	30	324	1128 s	0.92

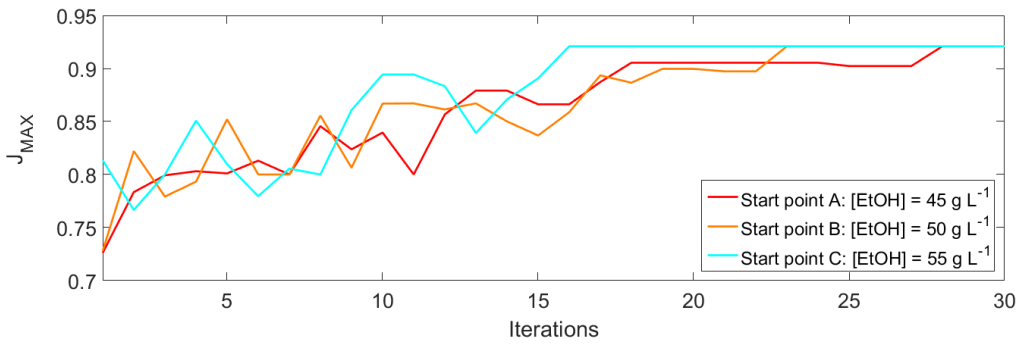

Figure 13. Simulated annealing objective function per iteration from 3 initial points (W_t = 90%, W_E = 10%).

4.3.2 EXHAUSTIVE EVALUATION

The exhaustive evaluation of all (175,000) candidate temperature manipulation profiles has been pursued in order to validate the Simulated Annealing (SA) algorithm constructed and results obtained: the same objective function given in Eq. (29) has been used in order to calculate J values for every single temperature profile, using the same component weights.

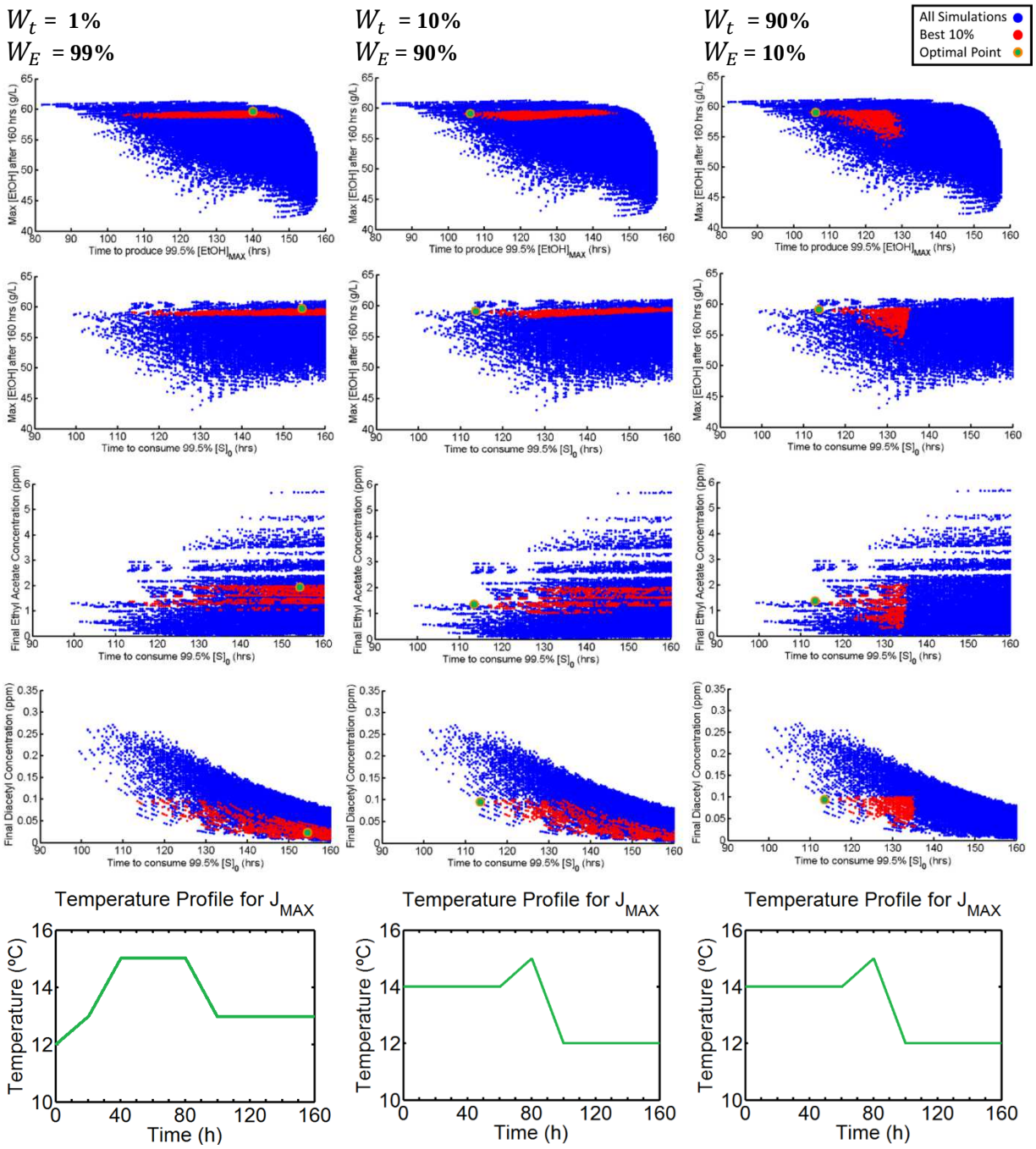

Figure 14. Exhaustive optimisation results for varying J-function component weights.

Figure 14 illustrates the top 10% (red points) and the optimal (green point) product quality combinations achieved, respectively, superimposed on the entire attainable envelope (blue points). The optimal points identified are precisely those determined via simulated annealing, which is however a lot more efficient as it performs only a minute fraction of objective function evaluations.

Both simulated annealing (SA) and exhaustive evaluation (EE) approaches arrive at the same temperature profiles to maximise the objective function of Eq. (29) and satisfy the the constraints of Eqs. (30-31). For the vast majority of objective function weight allocation values, the optimal temperature profile determined remains the same (Fig. 15); its performance is compared to the current industrial (WEST Beer) manipulation in Table 8. The batch time reduction achieved is spectacular (12.3%), and it is accompanied by a small desirable increase in final ethanol concentration; while both by-product concentrations do increase marginally as well, they are well below tolerable thresholds and do not affect flavour.

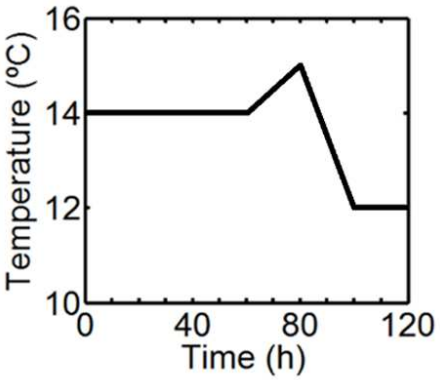

Figure 15. Optimal temperature profile.

Table 8. Optimal fermentation profile performance.

Parameter	**Units**	**Existing manipulation**	**New profile** (Figure 14)
Fermentation time	hrs	129.5	113.5
Ethanol concentration	g L^{-1}	59.0	59.1
EA concentration	ppm	1.16	1.35
DY concentration	ppm	0.06	0.09

5. CONCLUSIONS

Promising fermentation process improvements are highly desirable in beer production, as a reduction in batch time for fermentation directly translates into higher plant throughput and profitability. Beer production appears to be a simple process, requiring only four ingredients and a sequence of established processing steps. However, it is a very complex chemical system with a vast number of reactions, many of which are still not quantitatively understood. Predicting the effect of operational modifications is not straightforward: historical efforts to improve productivity are based on empirical approaches, but varying experimental conditions and observing their effects is a laborious, costly and inefficient procedure. Recent research

studies have considered all key species and relied on suitable reduced-order dynamic models toward dynamic simulation, optimisation and control of the fermentation process.

This paper employs a widely validated beer fermentation model (de Andrés-Toro et al., 1998) which has been implemented in order to predict species concentration evolution for any set of initial and operating (temperature profile) conditions; the code has been successfully validated computationally against profiles previously published by other research groups. A range of operating temperature profiles published in the literature have been simulated, and their performance has been assessed using several quantitative indicators of fermentation performance (final concentrations of ethanol and aromatic by-products, batch production time). The trade-off between product quality and batch time is evident: results clearly show that aromatic by-product concentrations can be reduced during longer fermentation. This balance of operational objectives makes the determination of a single optimal temperature a very challenging problem: the latter depends on each brewer's target product composition, and arbitrary target variable weighting appears a popular but also questionable methodology.

A simulation-based optimisation procedure has been developed, facilitating the comparison of over 175,000 unique scenarios against the current industrial temperature manipulation. Each scenario represents a unique temperature profile, generated using suitable constraints which are representative of manipulations that are indeed applicable to the real process. This procedure also ensures that the degree of domain discretisation only produces temperature profiles which are implementable, without the need for a secondary smoothing process. A small sacrifice in ethyl acetate concentration (to a level not exceeding the acceptable beer flavour threshold) allows for a considerable reduction of batch time, while maintaining the ethanol and diacetyl concentration levels close to those achieved in the industrial (WEST Beer) process. Three unique novel manipulations have been identified, each with the potential to drastically reduce batch time (by up to 15 hours), with no discernible impact on beer flavour and quality.

A simulated annealing (SA) algorithm has also been developed in order to rapidly investigate the entire solution space and determine the optimal temperature manipulation profile which maximises a weighted objective function considering both ethanol maximisation and batch time minimisation, subject to explicit by-product constraints; several weight assignment cases have been solved and presented, indicating limited result sensitivity to weight value allocation.

A novel temperature profile (with a conspicuous heating peak) has been discovered, indicating that this non-trivial manipulation can reduce fermentation time by 16 hours, but also increase ethanol concentration and maintain by-product concentrations below threshold values. Experimental validation of these extremely encouraging model predictions against the industrial (WEST Beer) process has been advised as essential, in order to quantify and evaluate attainable benefits, but also assess the impact of underlying modelling assumptions (especially with respect to vessel temperature distribution and yeast biochemical behaviour).

ACKNOWLEDGEMENTS

The authors gratefully acknowledge the financial support of the Eric Birse Charitable Trust for a Birse Doctoral Fellowship awarded to Mr. A.D. Rodman, and that of the Engineering and Physical Sciences Research Council (EPSRC) via funding from an Impact Acceleration Account (IAA) administered by Edinburgh Research & Innovation (ERI). Moreover, they express their thanks to Mrs Hilary Jones, Mr Simon P. Roberts and Mr Udo Zimmermann (WEST Beer) for consistent encouragement and inspiring discussions throughout this project.

NOMENCLATURE

Symbol	Description	Units
$(\ )_0$	Initial condition	-
A_i	Arrhenius constant (species i)	K
B_i	Arrhenius constant (species i)	K^{-1}
C_i	Concentration (species i)	$g\ L^{-1}$
X_{act}	Active biomass concentration	$g\ L^{-1}$
X_{dead}	Dead biomass concentration	$g\ L^{-1}$
X_{inc}	Inoculated biomass concentration	$g\ L^{-1}$
X_{lag}	Latent biomass concentration	$g\ L^{-1}$
X_{sus}	Suspended biomass concentration	$g\ L^{-1}$
Y_{EA}	Ethyl acetate production stoichiometric factor	$g\ L^{-1}$
k_e	Ethanol affinity constant	$g\ L^{-1}$
k_s	Sugar affinity constant	$g\ L^{-1}$
k_x	Biomass affinity constant	$g\ L^{-1}$
t_{lag}	Length of fermentation lag phase	h
μ_{AB}	Diacetyl consumption rate	$g^{-1}\ h^{-1}\ L$
μ_{DT}	Specific cell death rate	h^{-1}
μ_{DY}	Diacetyl growth rate	$g^{-1}\ h^{-1}\ L$
μ_E	Ethanol production rate	h^{-1}
μ_L	Specific cell activation rate	h^{-1}
μ_S	Sugar consumption rate	h^{-1}
μ_{SD}	Specific dead cell settling rate	h^{-1}
μ_x	Specific cell growth rate	h^{-1}
M	Discrete time points	-
N	Discrete temperature points	-
T	Fermenter temperature	K
P	Fermenter top pressure	bar
f	Fermentation inhibition factor	$g\ L^{-1}$
t	time	h
CO_2	Carbon dioxide	-
DY	Diacetyl	-
E	Ethanol	-
EA	Ethyl Acetate	-
S	Sugar	-

LITERATURE REFERENCES

1. Akinlabi, C. O., Gerogiorgis, D. I., Georgiadis, M. C., Pistikopoulos, E.N., 2007. Modelling, design and optimisation of a hybrid psa-membrane gas separation process. *Computer-Aided Chemical Engineering*, **24**, 363-370.
2. Angelopoulos, P. M., Gerogiorgis, D. I., Paspaliaris, I., 2013. Model-based sensitivity analysis and experimental investigation of perlite grain expansion in a vertical electrical furnace. *Industrial, Engineering Chemistry Research*, **52**, 17953-17975.
3. Angelopoulos, P. M., Gerogiorgis, D. I., Paspaliaris, I., 2014. Mathematical modeling and process simulation of perlite grain expansion in a vertical electrical furnace. *Applied Mathematical Modelling*, **38**, 1799-1822.
4. Arnold, J.P., 1911. Origin and history of beer and brewing: *From prehistoric times to the beginning of brewing science and technology; a critical essay*, Alumni Association of the Wahl-Henius Institute of Fermentology.
5. Boulton, C., Quain, D., 2008. *Brewing yeast and fermentation*, Wiley.
6. Carrillo-Ureta, G., 1999. *Optimal control of a fermentation process.* City University.
7. Carrillo-Ureta, G., Roberts, P., Becerra, V., 2001. Genetic algorithms for optimal control of beer fermentation. *Proceedings of the 2001 IEEE International Symposium on Intelligent Control 2001 (ISIC'01)*, pp. 391-396.
8. Corrieu, G., Trelea, I. C., Perre, B. 2000. On-line estimation and prediction of density and ethanol evolution in the brewery. *MBAA Technical Quarterly*, 173-181.
9. de Andrés-Toro, B., Girón-Sierra, J. M., López-Orozco, J. A., Fernández-Conde, C., Peinado, J. M., García-Ochoa, F. 1998. A kinetic model for beer production under industrial operational conditions. *Mathematics and Computers in Simulation*, **48**, 65-74.
10. de Andrés-Toro, B., Giron-Sierra, J., Fernandez-Blanco, P., Lopez-Orozco, J., Besada-Portas, E. 2004. Multiobjective optimization and multivariable control of the beer fermentation process with the use of evolutionary algorithms. *Journal of Zhejiang University Science*, **5**, 378-389.
11. Engasser, J. M., Marc, I., Moll, M. Duteurte, B., 1981. Kinetic modelling of beer fermentation. Proceedings of the 18th Congress of the European Brewery Convention, Copenhagen, pp. 579-586.
12. Gee, D.A., Ramirez, W.F., 1988. Optimal temperature control for batch beer fermentation. *Biotechnology and Bioengineering*, **31**, 224-234.
13. Gee, D.A., Ramirez, W.F., 1994. A flavour model for beer fermentation. *Journal of the Institute of Brewing*, **100**, 321-329.
14. Gerogiorgis, D., Ydstie, B., Seetharaman, S. 2001. A steady state electrothermic simulation analysis of a carbothermic reduction reactor for the production of aluminium. *Comput. Modeling of Materials, Minerals and Metals Processing*, 273-282.
15. Gerogiorgis, D.I., Ydstie, B.E., 2005. Multiphysics CFD modelling for design and simulation of a multiphase chemical reactor. *Chemical Engineering Research and Design*, **83**, 603-610.
16. Gerogiorgis, D. I., Georgiadis, M., Bowen, G., Pantelides, C.C., Pistikopoulos, E.N. 2006. Dynamic oil and gas production optimization via explicit reservoir simulation.
17. Gerogiorgis, D.I., Barton, P.I., Steady-state optimisation of a continuous pharmaceutical process, *Computer-Aided Chemical Engineering*, **27**, 927-932.
18. Gonzalez, O.R., et al., 2007. Parameter estimation using Simulated Annealing for S-system models of biochemical networks. *Bioinformatics* **23**(4), 480-486.

19. Guido, L., Rodrigues, P., Rodrigues, J., Goncalves, C., Barros, A., 2004. The impact of the physiological condition of the pitching yeast on beer flavour stability: An industrial approach. *Food chemistry*, **87**, 187-193.
20. Hanke, S., Ditz, V., Herrmann, M., Back, W., Becker, T., Krottenthaler, M., 2010. Influence of ethyl acetate, isoamyl acetate and linalool on off-flavour perception in beer. *Brew. Sci*, **63**, 94-99.
21. Hedengren, J., 2015. Optimization Techniques in Engineering, accessed 12 December 2015, < http://apmonitor.com/me575/index.php/Main/HomePage>
22. Hough, J.S., Stevens, R., Young, T.W., 1982. *Malting and brewing science: Hopped wort and beer*, Springer Science, Business Media.
23. Hudson, J.R., Birtwistle, S. E. 1966. Wort-boiling in relation to beer quality. *Journal of the Institute of Brewing*, **72**, 46-50.
24. Izquierdo-Ferrero, J.M., Fernández-Romero, J.M., De Castro, M.D.L., 1997. On-line flow injection–pervaporation of beer samples for the determination of diacetyl. *Analyst*, **122**, 119-122.
25. Jolliffe, H.G., Gerogiorgis, D.I., 2015a. Plantwide design and economic evaluation of two continuous pharmaceutical manufacturing (CPM) cases: Ibuprofen and artemisinin. *Proceedings of the Joint 12th International Conference on Process Systems Engineering and 25th European Symposium on Computer-Aided Process Engineering* (PSE 2015-ESCAPE 25), Elsevier, Amsterdam.
26. Jolliffe, H.G., Gerogiorgis, D.I., 2015b. Process modelling and simulation for continuous pharmaceutical manufacturing of ibuprofen. *Chemical Engineering Research and Design*, **97**, 175-191.
27. Kirkpatrick, S., 1983. Optimization by simulated annealing. *Journal of statistical physics*, **34**(5-6) 975-986.
28. Lee, F.C., Rangaiah, G.P., Ray, A.K., 2007. Multi-objective optimization of an industrial penicillin V bioreactor train using non-dominated sorting genetic algorithm. *Biotechnology and Bioengineering*, **98**(3), 586-598.
29. Liu, P., Gerogiorgis, D.I. and Pistikopoulos, E.N., 2007. Modelling, investment planning and optimisation for the design of a polygeneration energy system, *Computer-Aided Chemical Engineering*, **24**, 1095-1102.
30. Rehm, J., Uuml, R., Rehn, N., Room, R., Monteiro, M., Gmel, G., Jernigan, D., Frick, U., 2003. The global distribution of average volume of alcohol consumption and patterns of drinking. *European addiction research*, **9**, 147-156.
31. Research and Markets, R. A. 2013. *Analyzing the Global Beer Industry.*
32. Schaber, S.D., Gerogiorgis, D.I., Ramachandran, R., Evans, J.M., Barton, P.I., Trout, B.L. 2011. Economic analysis of integrated continuous and batch pharmaceutical manufacturing: A case study. *Industrial, Engineering Chemistry Research*, **50**, 10083-10092.
33. Singh, V., Khan, M., Khan, S. and Tripathi, C.K.M., 2009. Optimization of actinomycin V production by Streptomyces triostinicus using artificial neural network and genetic algorithm. *Applied microbiology and biotechnology*, **82**(2), 379-385.
34. Southby, E. R. 1885. *A Systematic Handbook of Practical Brewing.*
35. Stassi, P., Rice, J. F., Munroe, J. H., Chicoye, E., 1987. Use of CO_2 evolution rate for the study and control of fermentation. *MBAA Tech. Q.*, **24**, 44-50.
36. Taras, S. and Woinaroschy, A., 2011. Simulation and multi-objective optimization of bioprocesses with Matlab and SuperPro Designer using a client–server interface. *Chemical Engineering Transactions*, **25**, 207-212.

37. Trelea, I. C., Titica, M., Landaud, S., Latrille, E., Corrieu, G., Cheruy, A., 2001. Predictive modelling of brewing fermentation: From knowledge-based to black-box models. *Mathematics and Computers in Simulation*, **56**, 405-424.
38. Vanderhaegen, B., Neven, H., Verachtert, H., Derdelinckx, G., 2006. The chemistry of beer aging – a critical review. *Food Chemistry*, **95**, 357-381.
39. Xiao, J., Zhou, Z.-K., Zhang, G.-X., 2004. Ant colony system algorithm for the optimization of beer fermentation control. *Journal of Zhejiang University Science*, **5**, 1597-1603.